AD-A146 490 WAVELENGTH CODED IMAGE TRANSMISSION AND HOLOGRAPHIC OPTICAL ELEMENTS..(U) MINNESOTA UNIV MINNEAPOLIS DEPT OF ELECTRICAL ENGINEERING S K CASE 20 AUG 84 1/1

UNCLASSIFIED UM-ARO-AFOSR-1 ARO-17612.12-PH F/G 20/6 NL

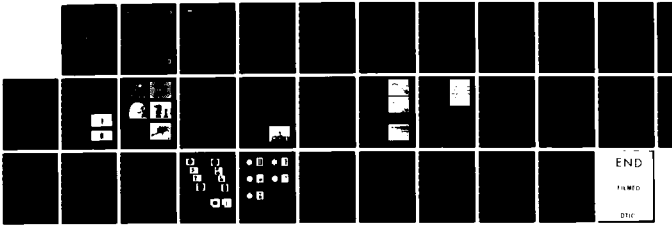

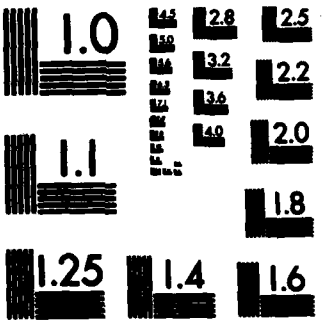

MICROCOPY RESOLUTION TEST CHART

ARO 17612.12-PH

Report UM-ARO-AFOSR-1

FINAL TECHNICAL REPORT

Feb. 1, 1981 - Apr. 30, 1984

WAVELENGTH CODED IMAGE TRANSMISSION

AND

HOLOGRAPHIC OPTICAL ELEMENTS

Steven K. Case, Principle Investigator

Department of Electrical Engineering
University of Minnesota
123 Church Street Southeast
Minneapolis, MN 55455

August 20, 1984

Research supported by the
Army Research Office
and
Air Force Office of Scientific Research
under Grant No. DAAG 29-81-K-0033

Approved for Public Release
Distribution Unlimited

UNCLASSIFIED
SECURITY CLASSIFICATION OF THIS PAGE (When Data Entered)

MASTER COPY - FOR REPRODUCTION PURPOSES

REPORT DOCUMENTATION PAGE

READ INSTRUCTIONS BEFORE COMPLETING FORM

1. REPORT NUMBER [redacted]12.12-PH	2. GOVT ACCESSION NO. N/A
3. RECIPIENT'S CATALOG NUMBER N/A	
4. TITLE (and Subtitle) Wavelength Coded Image Transmission and Holographic Optical Elements	5. TYPE OF REPORT & PERIOD COVERED Final Technical Report 2/1/81 - 4/30/84
	6. PERFORMING ORG. REPORT NUMBER UM-ARO-AFOSR-1
7. AUTHOR(s) Steven K. Case	8. CONTRACT OR GRANT NUMBER(s) DAAG 29-81-K-0033
9. PERFORMING ORGANIZATION NAME AND ADDRESS Electrical Engineering Department University of Minnesota Minneapolis, MN 55455	10. PROGRAM ELEMENT, PROJECT, TASK AREA & WORK UNIT NUMBERS
11. CONTROLLING OFFICE NAME AND ADDRESS U. S. Army Research Office Post Office Box 12211 Research Triangle Park, NC 27709	12. REPORT DATE 8/20/84
	13. NUMBER OF PAGES 32
14. MONITORING AGENCY NAME & ADDRESS (if different from Controlling Office) as above	15. SECURITY CLASS. (of this report) Unclassified
	15a. DECLASSIFICATION/DOWNGRADING SCHEDULE

16. DISTRIBUTION STATEMENT (of this Report)

Approved for public release; distribution unlimited.

17. DISTRIBUTION STATEMENT (of the abstract entered in Block 20, if different from Report)

NA

18. SUPPLEMENTARY NOTES

The view, opinions, and/or findings contained in this report are those of the author(s) and should not be construed as an official Department of the Army position, policy, or decision, unless so designated by other documentation.

19. KEY WORDS (Continue on reverse side if necessary and identify by block number)

Fiber Optics
Image Transmission
Wavelength Multiplexing
Image Reconstruction
Polychromatic Lasers
Multifacet Holograms
Dichromated Gelatin
Holographic Optical Elements

20. ABSTRACT (Continue on reverse side if necessary and identify by block number)

The results of a three year optics research program are described. Research was initially performed on wavelength coded image transmission. The goal of the program was to study various methods and systems for encoding object information in a wavelength multiplexed form so that the various wavelengths could be transmitted through a non-imaging media such as fog or a fiber optic and later spatially repositioned to reassemble an image of the original object. Such a system could be used to transmit image formation at higher data rates and/or to transmit images through fewer optical channels.

DD FORM 1 JAN 73 1473 EDITION OF 1 NOV 65 IS OBSOLETE

UNCLASSIFIED
SECURITY CLASSIFICATION OF THIS PAGE (When Data Entered)

(20. continued)

During the second year, the program was augmented to include research on a new type of holographic optical element called a multifacet hologram. Such holograms consist of a large number of small, adjacent holograms (facets) which collectively diffract light to produce a desired output. These elements share some of the flexibility advantageous to Computer Generated Holograms with the high optical efficiency inherent in interferometrically recorded volume holograms. A computer controlled recording system was built to fabricate these elements. A number of space-variant image operations not possible with conventional optics were demonstrated using multi-facet holograms.

This research program has produced 16 publications and 12 presentations in addition to several M.S. and Ph.D. dissertations.

Table of Contents

Abstract

The results of a three year optics research program are described. Research was initially performed on wavelength coded image transmission. The goal of the program was to study various methods and systems for encoding object information in a wavelength multiplexed form so that the various wavelengths could be transmitted through a non-imaging media such as fog or a fiber optic and later spatially repositioned to reassemble an image of the original object. Such a system could be used to transmit image information at higher data rates and/or to transmit images through fewer optical channels.

During the second year, the program was augmented to include research on a new type of holographic optical element called a multifacet hologram. Such holograms consist of a large number of small, adjacent holograms (facets) which collectively diffract light to produce a desired output. These elements share some of the flexibility advantageous to Computer Generated Holograms with the high optical efficiency inherent in interferometrically recorded volume holograms. A computer controlled recording system was built to fabricate these elements. A number of space-variant image operations not possible with conventional optics were demonstrated using multi-facet holograms.

This research program has produced 16 publications and 12 presentations in addition to several M.S. and Ph.D. dissertations.

1. RESEARCH OBJECTIVES AND RESULTS

1.1 Introduction to Wavelength Coded Image Transmission

A optical fiber represents a single communication channel and as such is not ideally suited for the parallel transmission of 2-D image information. Image information can be transmitted through optical fibers by assembling a bundle of parallel fibers, each of which carries one pixel of information, as in an endoscope; or by using time multiplexing to sequentially send pixel information, much as a television camera sequentially sends information to a TV monitor.

In this research program, we investigated ways in which points on an object could be illuminated with different wavelengths, enacting a position to wavelength encoding. The various wavelengths comprising the image can then propagate through a media which would not normally transmit 2-D images such as a fog or an optical fiber. Even though the light may be scattered on mixed during propagation, its wavelength remains unchanged so that the integrity of the image information remains. In the receiving portion of the system, the light is spatially rearranged on a wavelength basis in order to properly reassemble an image.

Several systems were built. One sent coded image information in parallel through a fiber. Such a system could potentially achieve very high data rates. Another system (reported at a National Fiber Optic conference in New Orleans) transmitted spectral information sequentially but required only a few fibers and completely passive optics at its distal end to transmit 2-D images at TV frame rates. A new "white laser" was developed for this program.

Technical results from this program are described by selected reprints in Section 1.3.

1.2 Multifacet Holographic Optical Elements

Diffractive optical elements are known to be desirable alternatives to conventional optical elements when size and weight are concerned. Holographic optical elements (HOEs) are often characterized as being computer generated or interferometrically recorded. Traditionally, computer generated holograms offer the greatest flexibility in the generation of arbitrary wavefronts but suffer from low optical efficiency. Interferometric HOEs usually have reduced flexibility, since they are often recorded with reasonably simple wavefronts such as spherical or plane waves, but can be recorded as volume holograms which exhibit nearly 100% optical efficiency. Of course, many qualifiers must be added to the above simplified categorizations. Nonetheless, our goal in this program was to combine some of the flexibility of computer generated HOEs with the high optical efficiency of interferometrically recorded HOEs. To accomplish this, we have built a computer controlled hologram recording system in which two Argon laser beams are used to expose one small portion of a dichromated gelatin film at one time. The laser beams can be incident on the film at arbitrarily prescribed angles (under computer control) and with a desired focal power. In this manner, each portion (facet) of the film can have arbitrary deflection capabilities. Taken collectively, a large number of small facets can be used to perform complex, space variant operations with high optical efficiency.

A number of optical elements have been demonstrated using this technique. Their functions include elements for: coordinate transformations, custom laser beam shaping, custom object illumination, laser beam scanners, focusing on curved substrates, and information encrypting. Elements could also be made for optical computing and optical interconnects.

A number of papers and presentations have resulted from research in this area. Selected reprints are contained in Section 1.4.

1.3 Selected papers

Wavelength coding for image transmission through aberrating media.

Fiber optic image transmission system with high resolution.

Polychromatic laser light source.

Wavelength coding for image transmission through aberrating media

S. K. Case

Department of Electrical Engineering, Minneapolis, Minnesota 55455

Received March 2, 1981

A wavelength-coded source is used for spectral encoding of a spatial signal. The signal is passed through an aberrating medium and then a spectral decoding filter. A high signal-to-noise ratio image is present in real time at the system output.

Introduction

The problem of viewing through aberrating media (e.g., fog) is important and has been the subject of considerable research.[1] Range gating[2,3] and angle scanning[4] are opto-electronic techniques using pulsed sources and detectors that only "look" for the image signal at the appropriate time and/or angle in order to reduce the signal contribution from scattered light. Various holographic techniques have also been used to compensate for static (spatially and temporally invariant) phase distortions introduced by an aberrating medium.[5-8]

Another holographic technique is useful in the presence of a temporally varying dispersive medium.[9-11] This technique discriminates against scattered light but requires large detector dynamic range since the scattered light produces a large bias that results in low signal-to-background ratio. Recent developments of this technique permit real-time readout,[12] and others permit white-light illumination for hologram recording.[13]

In this Letter, we show another technique for image transmission through aberrating media. Our demonstration uses simple, passive elements and produces high-contrast images in real time.

Wavelength-Coded Transmission

Our technique uses a wavelength-coded source to illuminate each object-resolution cell (pixel) with a different wavelength. In this manner spatial information is encoded into spectral information. Each spectral wavelength now propagates independently (i.e., without conversion to another wavelength—except for negligible Doppler shifts) through the aberrating medium. The medium may be stationary or moving. Decoding at the receiver is accomplished by passing the light through a spectrograph, which displays the proper wavelengths at the proper spatial positions so that the image is correctly reassembled. All the light that passes through the decoding spectrograph is used to produce the desired image, so the image contrast is high.

A compact experimental setup that can be used for one-dimensional objects is shown in Fig. 1. A beam of collimated white light is incident upon a wedge interference filter. This filter is such that at a given position x on the filter, only a narrow band of wavelengths is transmitted. The center wavelength of this band changes linearly with position x. Hence each resolution cell along the x axis of the object is illuminated with a different wavelength. The color-coded signal emerging from the object transparency propagates between the source and receiver. The lens is not necessary but may be used to increase light efficiency or permit imaging scaling. The aberrating medium is assumed to be in the transmission path. Decoding, at the receiver, is accomplished by passing the light through a second wedge interference filter, which transmits only the desired wavelengths at the proper spatial positions. In this example, if light of the wrong wavelength is incident at a particular position upon the decoding filter, it is simply reflected away and does not contribute to image contrast degradation.

Analysis

The white-light illumination in Fig. 1 is assumed to have a spectral-intensity distribution given by $L(\lambda)$. After passing through the encoding filter, the illumination is approximately described by

$$I_1(x_1,\lambda) = L(\lambda)\delta[\lambda - (\lambda_0 + ax_1)], \qquad (1)$$

where we have used a Dirac delta function and λ_0 is the wavelength transmitted at the center ($x_1 = 0$) of the filter. After passing through the one-dimensional object with transmittance $0(x_1)$, the signal is

$$I_2(x_1,\lambda) = L(\lambda)0(x_1)\delta[\lambda - (\lambda_0 + ax_1)]. \qquad (2)$$

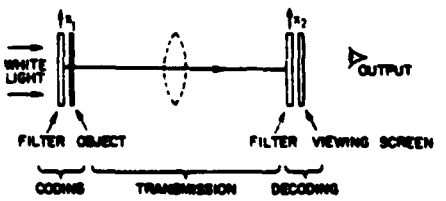

Fig. 1. Optical system.

The system impulse response $h(x_2,x_1)$ describes the propagation from the input to output planes. More specifically, it describes the intensity at output coordinate x_2 that is due to a unit intensity line source at input position x_1. The effects of the diffusing medium and the presence of any lenses will be accounted for in h. If the diffuse transmission medium has detail that is small compared with the object resolution and is reasonably isotropic, h can be considered approximately space invariant, so that the impulse response depends only on the difference in input and output coordinates

$$h(x_2,x_1) = h(x_2 - x_1). \tag{3}$$

The intensity just before the decoding filter is given by the superposition integral[14]

$$I_3(x_2,\lambda) = \int h(x_2 - x_1)L(\lambda)O(x_1) \times \delta[\lambda - (\lambda_0 + ax_1)]dx_1. \tag{4}$$

The decoding filter has transmittance

$$T(x_2,\lambda) = \delta[\lambda - (\lambda_0 + bx_2)], \tag{5}$$

so that the output intensity is

$$I_4(x_2,\lambda) = \delta[\lambda - (\lambda_0 + bx_2)]I_3(x_2,\lambda) \tag{6a}$$

$$= \int h(x_2 - x_1)L(\lambda)O(x_1) \times \delta[\lambda - (\lambda_0 + bx_2)]\delta[\lambda - (\lambda_0 + ax_1)]dx_1 \tag{6b}$$

$$= \int h(x_2 - x_1)L(\lambda)O(x_1) \times \delta\left[x_2 - \frac{a}{b}x_1\right]\delta[\lambda - (\lambda_0 + ax_1)]dx_1. \tag{6c}$$

As an illustration, we assume that the input consists of a narrow transparent slit centered at $x_1 = x_0$ in an opaque background, that the source has uniform spectral irradiance $L(\lambda) = 1$, and that the aberrating medium is such as to produce a band of output light of width X centered at $x_2 = x_1$. Neglecting scaling factors preceding the integral, Eq. (6c) becomes[14]

$$I_4(x_2,\lambda) = \int \text{rect}\left(\frac{x_2 - x_1}{X}\right)\delta(x_1 - x_0) \times \delta\left(x_2 - \frac{a}{b}x_1\right)\delta[\lambda - (\lambda_0 + ax_1)]dx_1 \tag{7a}$$

$$= \text{rect}\left(\frac{x_2 - x_0}{X}\right)\delta\left(x_2 - \frac{a}{b}x_0\right) \times \delta[\lambda - (\lambda_0 + ax_0)] \tag{7b}$$

$$= \text{rect}\left(\frac{\frac{a}{b}x_0 - x_0}{X}\right) \times \delta\left(x_2 - \frac{a}{b}x_0\right)\delta[\lambda - (\lambda_0 + ax_0)]. \tag{7c}$$

Equation (7c) indicates that the output image consists of a narrow slit at position $x_2 = (a/b)x_0$, with wavelength $\lambda = \lambda_0 + ax_0$. Because we have assumed the coding and decoding filters to be scaled differently ($a \neq b$), for sufficiently large values of x_0, the band of scattered light at the output will not be wide enough for light of wavelength $\lambda = \lambda_0 + ax_0$ to reach the area of transmission for that wavelength on the decoding filter. Thus, for $a > b$, the rect function in Eq. (7c) limits the field of view to

$$|x_0| \lesssim \frac{X}{2\left(\frac{a}{b} - 1\right)}. \tag{12}$$

The above analysis shows that the coding and decoding filters produce a new type of imaging system with magnification $M = a/b$ that does not require any lenses.

Experimental Results

The system shown in Fig. 1 was used with an imaging lens and identical coding and decoding filters ($a = b$). The input object consisted of two open slits in an opaque background. The wavelength-coded transmitted image seen at the output is shown in Fig. 2(a). A color photograph would show a spectrum across the image. An aberrating medium consisting of a piece of ground glass was then inserted between the object and image planes. The ratio of unscattered to scattered light was measured to be 1:1400. In spite of this, the high-contrast output image in Fig. 2(b) was obtained. The soft edges seen in this image are an artifact of the interference filters in which the passband for a particular wavelength has finite width and changes lateral position for different light-incidence angles.

For reference, the diffuser was left in place and the decoding filter removed so that the wavelength-mapping mechanism was no longer operative. This is equivalent to eliminating the delta function involving

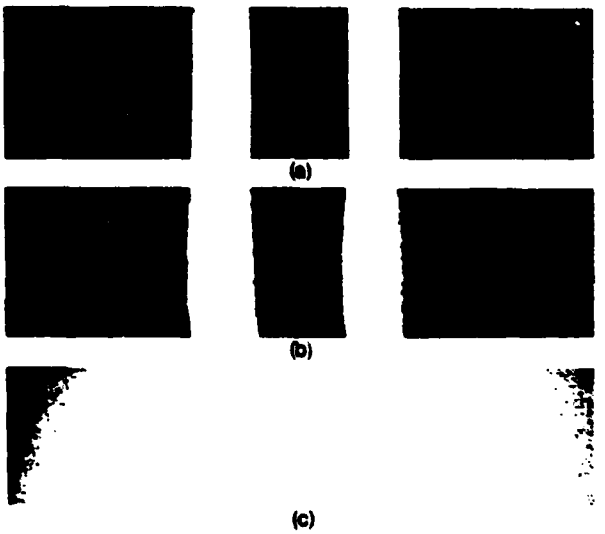

Fig. 2. (a) Wavelength-coded image in the absence of aberrating media. (b) wavelength-coded image with aberration (ground glass) inserted between object and image planes. (c) output image with ground glass present and final decoding filter removed so that wavelength-coded transmission is inoperative (for reference).

x_2 in Eq. (7b) so that we would now expect to see the broad diffusing function (impluse response) at the output. The output is shown in Fig. 2(c). The striking difference between Figs. 2(b) and 2(c) shows the validity of the wavelength-coding process for image transmission through aberrating media.

Conclusion

A wavelength-coding and -decoding system for one-dimensional image transmission through stationary and time-varying aberrating media has been demonstrated. The system uses only passive optics and produces high-contrast images in real time. Wavelength-coding methods can be extended to two dimensions.[15]

Experimental portions of this work were performed in the laboratory of A. Lohmann with the support of the Fulbright Commission. Partial support from the Engineering Foundation (grant RC-A-78-6D) and the Army Research Office–Air Force Office of Scientific Research (grant DAA29-81-K-0033) is also acknowledged.

References

1. *Digest of Topical Meeting on Optical Propagation through Turbulence, Rain, and Fog* (Optical Society of America, Washington, D.C., 1977).
2. S. Donati, Alta Freq. 43, 461 (1974).
3. D. G. Herzog, RCA Eng. 15, 58 (1970).
4. S. Donati and A. Sona, Opto-electronics 1, 89 (1969).
5. E. N. Leith and J. Upatnieks, "Holographic imagery through diffusing media," J. Opt. Soc. Am. 56, 523 (1966).
6. H. Kogelnik, "Holographic image projection through inhomogeneous media," Bell Syst. Tech. J. 44, 2451 (1965).
7. J. W. Goodman *et al.*, "Wavefront-reconstruction imaging through random media," Appl. Phys. Lett. 8, 311 (1966).
8. P. L. Ransom, "Proposal for holographic imaging through phase-distorting media without alignment," Opt. Lett. 5, 327 (1980).
9. K. A. Stetson, "Holographic fog penetration," J. Opt. Soc. Am. 57, 1060 (1967).
10. H. J. Caulfield, "Holographic imaging through scatterers," J. Opt. Soc. Am. 58, 276 (1968).
11. A. W. Lohmann and C. A. Shuman, "Holography through convective fog," Opt. Commun. 7, 93 (1973).
12. A. W. Lohmann and H. Schmalfuss, "Holography through fog. A new version," Opt. Commun. 26, 318 (1978).
13. B. J. Chang, J. S. Chang, and E. N. Leith, "Imaging through scattering media with an achromatic interferometer," Opt. Lett. 4, 118 (1979).
14. J. W. Goodman, *Introduction to Fourier Optics* (McGraw-Hill, New York, 1968).
15. H. O. Bartelt, "Transmission of two-dimensional images by wavelength multiplexing," Opt. Commun. 28, 45 (1979).

Reprinted from Applied Optics, Vol. 22, page 2029, July, 1, 1983

Fiber-optic image transmission system with high resolution

D. E. Hulsey and S. K. Case

A system has been designed and built for transmitting images of diffusely reflecting objects through optical fibers and displaying those images at a receiving station. Wavelength coding is used to reduce the number of fibers required for transmission while allowing transmission of >1000 pixels/fiber. The system is an optical/electronic hybrid which operates under computer control. A tunable dye laser is used for a high-brightness light source, and a CRT is used for the output image display. The system and its operation are described, and examples of results are shown.

I. Introduction

In a conventional fiber-optic imaging system, an image is focused onto the end of a 2-D coherent bundle of fibers. The image then propagates down the bundle with each resolvable point of the image traveling through an individual fiber. This is not the most efficient way to transmit information through optical fibers, however, because of their extremely high bandwidth and, therefore, high-information carrying capacity. The high bandwidth can be taken advantage of by using wavelength multiplexing. Alternately wavelength coding can be used to scan an object using only passive components at the end of a fiber-optic imaging system as described in this paper.

The first work on wavelength coding was done by Downes,[1] Lindenbald,[2] and Kartashev.[3] The basic idea is that different points on an object can be illuminated with different wavelengths of light so that spatial information is encoded as spectral information. The light may then be transmitted by any means, and no matter how aberrated it becomes in the process (e.g., transmitting through fog or an optical fiber), the spatial information can be retrieved by examining the spectral distribution of the light.

Several different imaging systems using wavelength coding have been demonstrated.[4-13] All previous systems have used a white light source for illumination. Wavelength coding has then been enacted by placing a wedge interference filter in contact with the objects, imaging the object through a dispersive element such as a prism or grating and onto a finite aperture, or imaging the source through a dispersive element before illuminating the object.

The resolution attainable with these systems is limited for practical reasons by the brightness of the light source. That is, the white light can only be divided into a limited number of resolvable wavelength bands with enough power in each band to be detectable.[12] For this reason, transparencies have been used as objects in previous systems to maximize light efficiency.

In this paper, we describe a new system that utilizes an extremely high brightness light source and has been designed to transmit high-resolution images of diffusely reflecting objects, while still allowing small detector integration times. Because transparencies are not needed, this system is not limited to 2-D objects but can also image 3-D objects.

II. Description of System

A. System Configuration and Operation

A diagram of the system can be seen in Fig. 1. The system is arranged so as to have a control station containing the light source, controls, detectors, processor, and display. The remainder of the system is a remote probe for viewing a distant object, consisting mostly of a spectrometer with two light paths, one for illumination light and one for receiving light reflected from the object. Illumination light is sent from the control station to the probe via a single-mode optical fiber. Returning optical signals from the probe are also transmitted to the control station by optical fibers (multimode, 50-μm core).

In designing a system for viewing diffusely reflecting objects, one must consider that a much lower fraction of light can be collected from a diffusely reflecting object as compared with the light transmitted through a transparency because of the loss of directionality of the illumination light. Therefore, a much brighter light

The authors are with University of Minnesota, Electrical Engineering Department, Minneapolis, Minnesota 55455.
Received 26 July 1982.
0003-6935/83/132029-05$01.00/0.

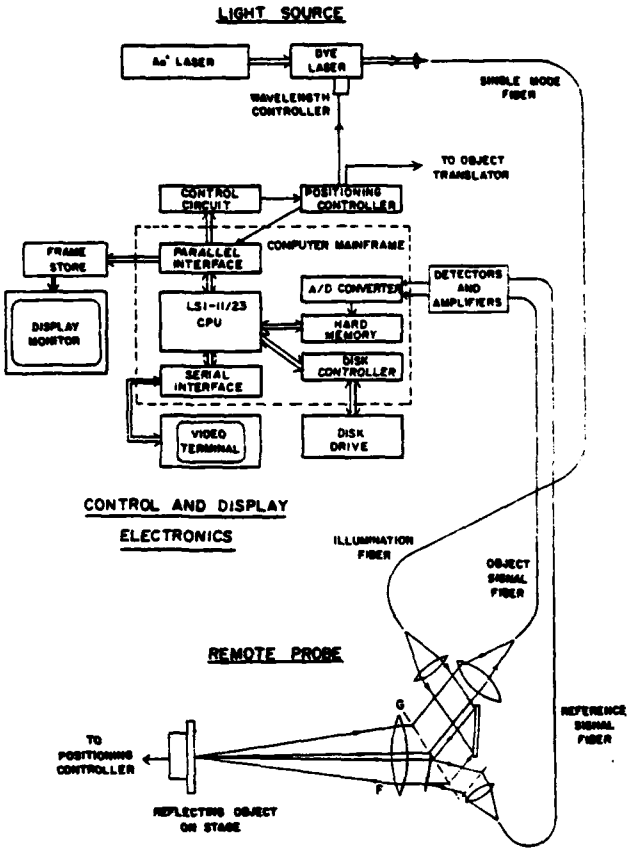

Fig. 1. Wavelength coded image transmission system.

source is needed for our system than was needed previously. The light source used is a tunable dye laser which is temporally scanned through its emission spectrum to simulate a high-brightness polyspectral source. This light source possesses all the desirable properties of a laser such as the ability to focus its entire output into a fiber for remote delivery and also is polychromatic so that it can be used for white light operations such as wavelength coded image transmission.

The operation of the entire system is as follows. The dye laser is set at a given wavelength via computer control. Light from the dye laser is sent to the remote probe by a single-mode fiber where it is collimated, deflected according to wavelength by a dichromated gelatin grating G, and focused onto one point of the object. The light reflected from the object is collimated, again deflected by G, and focused onto the object signal fiber. A small fraction of the illumination light is returned to the control station to act as an irradiance reference signal. This reference light is also doubly diffracted so as to account for any wavelength-dependent diffraction efficiency in the gratings.

At the control station, the two light signals are detected, amplified, and digitized by the computer. The computer normalizes the object signal by use of the reference signal and stores the pixel value in an array. Under computer control the dye laser output wavelength is incremented so that a new object pixel is illuminated and read. The process is repeated until the dye laser scans through its entire wavelength range, thus scanning the object with a point of light while the computer reads the values of the pixels along one horizontal line. In this experiment, the computer then moves the object vertically by the width of one image line, and the dye laser scans to read this line. The process is repeated until the entire image has been read and stored. The image data are then transferred to a digital frame store for subsequent display on a TV monitor. Because our object was translated to view different object lines, the probe is not totally passive. This objection can be easily removed, however, by adding a cylindrical lens to the illumination system so than an entire vertical line is illuminated on the object at one time and by adding a corresponding vertical row of return signal fibers which can be read by a linear photodiode array. Thus only one scan of the dye laser spectrum would be required to gather an entire image, and the probe would be entirely passive.

Because a scanning dye laser is used as the light source, this system does not truly use parallel wavelength multiplexing as is the case with previous wavelength coding systems since our pixel information is transmitted serially. Instead this system uses wavelength coding to scan object lines using passive optical components in the remote probe.

In addition to the high brightness of this source, which leads to good image resolution[12] as described in the next section, there are other advantages to using the dye laser. Since this source emits only one narrow wavelength band at a time, all the laser output power is directed into one object pixel at one time. This high power/pixel can be coupled to a short sampling or integration time for the detector to reduce noise. The power/pixel for our dye laser system is thus nearly independent of the image resolution where for a white light source, increased resolution is obtained by dividing the available power among more pixels thereby reducing the power/pixel so that longer detector integration times (with associated noise) are required. The average source brightness for our system is $\sim 10^4$ higher than that for the arc lamp used in the previous paper.[12] Of course, fewer detectors are also required with the serial wavelength scheme.

B. Resolution Calculations

The resolution of the remote probe is determined by the ratio of the length of the scan line to the width of the illuminating focal spot on the object. The length of the scan line L is given by[14]

$$L = 2F \tan \frac{\Delta\theta_{out}}{2}, \quad (1)$$

where F is the focal length of the lens which focuses the light onto the object, and $\Delta\theta_{out}$ is the range of angles into which the various dye laser output wavelengths are deflected by the diffraction grating. From the scaler diffraction equation,

$$\Delta\theta_{out} = \sin^{-1}(\sin\theta_{in} - \lambda_1 f) - \sin^{-1}(\sin\theta_{in} - \lambda_2 f), \quad (2)$$

where θ_{in} is the incidence angle of the illumination beam on the diffraction grating, f is the frequency of the diffraction grating, and λ_1 and λ_2 are the respective minimum and maximum wavelengths emitted by the dye laser.

For one given wavelength, the illuminating focal spot size at the object surface would have a certain width W_1 given by the diameter (between $1/e^2$ intensity points) of the output light from the single-mode fiber ($\sim 5\ \mu m$) multiplied by the magnification of the probe imaging system.

That width, however, is increased because the output of the dye laser actually contains a small band of wavelengths $\Delta\lambda$, which is dispersed by the diffraction grating. The dispersion width W_2 of the illumination spot can be calculated by using Eq. (1) and differentiating the scaler diffraction equation to get[14]

$$W_2 = 2F \tan \frac{\Delta\theta'_{out}}{2}, \quad (3)$$

where

$$\Delta\theta'_{out} = \frac{f\Delta\lambda}{\sqrt{1 - (\sin\theta_{in} - \lambda f)^2}}. \quad (4)$$

The power spectrum of the small band of wavelengths $\Delta\lambda$ from the dye laser is not flat and does not have sharp cutoffs. Therefore, the point spread function from the dispersion of this band is assumed to be a Gaussian function with W_2 being the distance between the $1/e^2$ points. To find the actual width of the focal spot on the object, this point spread function must be convolved with the undispersed image function of Gaussian width W_1. The convolution of two Gaussian functions of width W_1 and W_2 gives another Gaussian function with width W' given by

$$W' = \sqrt{W_1^2 + W_2^2}. \quad (5)$$

Therefore, the number of resolvable pixels in one scan line is given by L/W' assuming there are no aberrations in the system to increase the illumination spot size.

For our system, $L/W' = 1270$ pixels. Since our frame store can only store and display 256 pixels/line, our electronic system cannot display the full resolution capability of the optical system. For this reason, the data for each image pixel were actually obtained by reading data from several closely spaced points along an object scan line and averaging the results. This averaging conveniently served to reduce noise in the system.

The major source of noise is the speckle pattern in the light that reflects off the object due to using coherent illumination. This speckle pattern is invariably sampled by the finite apertures within the optical system. The effects of speckle noise are reduced by the incoherent averaging described above.

C. Imaging 3-D Objects

In addition to the high resolution afforded by our system, a major advantage is obtained in that it can transmit images of opaque 3-D objects. To transmit the image of a 3-D object and to perceive it as a 3-D object, it would be desirable to be able to collect information about the contours of the object. One method is to observe shadows on the object. That method cannot be applied in this case, however, since the angle at which the object is illuminated is so close to that at which it is observed.

In our case contours are seen because of the angular dependence of reflectivity of the object surface. Most diffusively reflecting surfaces do not reflect a beam of light uniformly into all directions. Instead the amount of light reflected into each direction varies so that the direction with the most reflected light is the direction in which specular reflection would go. Thus, if a surface is illuminated at a fixed angle and observed from a fixed angle, the amount of reflected light observed depends on the angle of the surface. Surfaces closest to normal to the bisector of the illumination and observation directions are brightest, and the surfaces gradually get darker as they move away from that angle. This effect is used in our system to observe 3-D objects.

III. Results

An example of the signals produced by the system in transmitting one line of an image is shown in Fig. 2. Figure 2 is a plot of the reference signal (dotted line) and object signal (solid line), which was read by the computer as one line of a star target (see Fig. 5) was scanned by the system. The bell shaped envelope of the reference signal is indicative mostly of the gain curve of the dye laser as a function of wavelength. Figure 3 shows

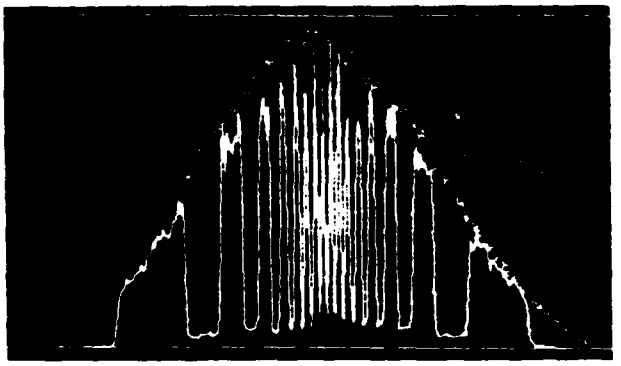

Fig. 2. Reference signal (dotted lines) and object signal (solid line) plotted vs position along one line of a star target.

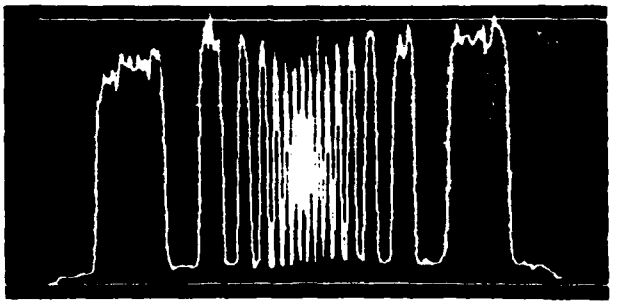

Fig. 3. Normalized object signal from data in Fig. 2.

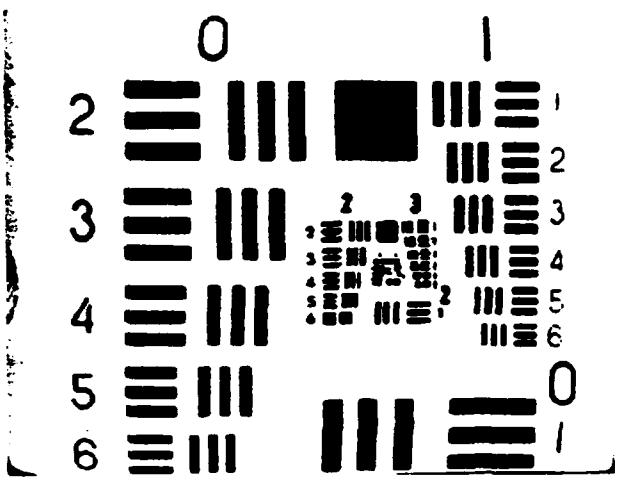

Fig. 4. Transmitted image of Air Force resolution target.

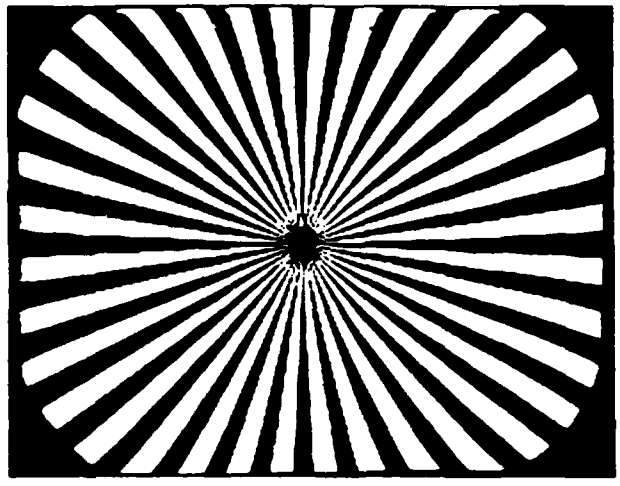

Fig. 5. Transmitted image of a star target.

Fig. 6. Transmitted gray tone image.

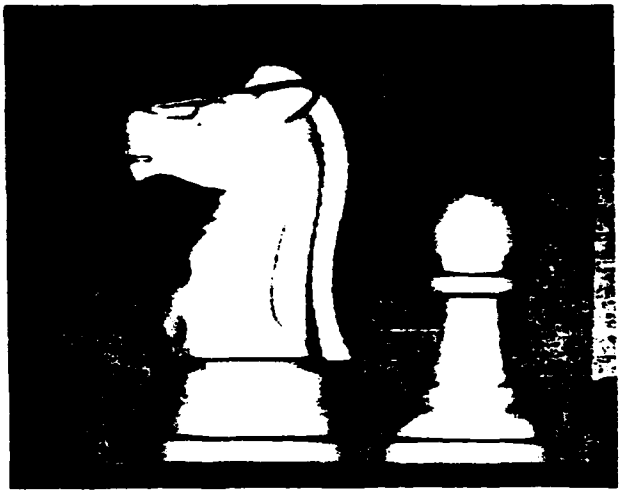

Fig. 7. Transmitted image of a 3-D opaque object.

a plot of the normalized data obtained from the ratio of the object signal to reference signal for a scan along the same line of the star target. This is thus a plot of image intensity vs horizontal position along one line of the object and is the data sent to the frame store for display. The two straight lines above and below the plot indicate the limits of the gray levels which can be stored and displayed.

Figures 4–8 show images that were transmitted by the system. Figures 4 and 5 illustrate the resolution with which images can be transmitted by the system. The objects that gave these images were photographs of an Air Force resolution target and a star target, respectively. Figure 6, also the transmitted image of a photograph, demonstrates the ability of the system to transmit accurately images with gray tones. The high resolution and uniform image brightness across the picture are a result of the use of the dye laser and subsequent computer image processing. Figures 7 and 8

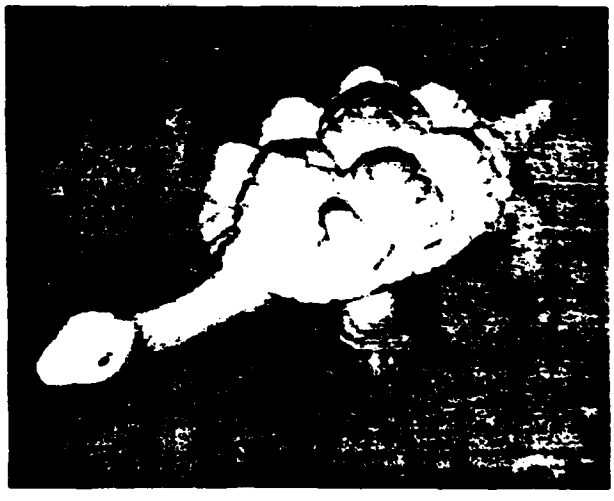

Fig. 8. Transmitted image of another 3-D opaque object.

are the transmitted images of 3-D objects. The soft edges on the pawn in Fig. 7 are seen because the illumination light is incident there at near grazing incidence angle and is not strongly scattered back to the receiving optics. The choice of object in Fig. 8 is not indicative of the pace of our research efforts.

IV. Conclusion

The choice to use wavelength coding for image transmission is predicated on the desire to achieve one or more of three goals: (1) to take advantage of the potentially high data rates associated with wavelength multiplexing; (2) to reduce the number of fibers required for image transmission; (3) to obtain higher resolution images than possible with commercial coherent fiber bundles. One also has to assume that the system would be used in an environment that precludes the use of a conventional TV camera because of excessive rf interference, radiation damage, electrical hazard, or physical size.

The optoelectronic imaging system described in this paper satisfies catagories (2) and (3). The system in its present configuration is relatively slow because the wavelength coded information from each line is sent serially, and subsequent image lines are also serially transmitted. However, by using a single column of optical fibers (one for each row in the image), the data rate increases and the remote probe becomes entirely passive. In addition, using electrooptic tuning for rapid scanning of the dye laser through its spectrum allows one to use a normal TV camera as a detector to display real-time images.[15]

Thus a modified version of our system will yield high-resolution images through a small number of fibers. The use of few fibers (i.e., one column) is of particular importance for transmission of images over distances greater than a few meters when 2-D coherent fiber bundles are not available or where space limitations make it desirable to use a smaller number of fibers.

The authors appreciate support from ARO/AFOSR grant DAAG29-81-K-0033. The data in this paper are taken from D. Husley's M.S. thesis completed in June 1982.

References

1. A. J. Downes, British Patent 129,747 (1918).
2. N. E. Lindenblad, U.S. Patent 2,443,258 (1948).
3. A. I. Kartashev, Opt. Spectrosc. **9**, 204 (1960).
4. S. K. Case, Opt. Lett. **6**, 311 (1981).
5. H. O. Bartelt, Opt. Commun. **27**, 365 (1978).
6. J. D. Armitage, A. Lohmann, and D. P. Paris, Jpn. J. Appl. Phys. **4**, 273 (1965).
7. H. O. Bartelt, Opt. Commun. **28**, 45 (1979).
8. M. L. Polanyi, J. Opt. Soc. Am. **56**, 1454 (1966).
9. C. J. Koester, J. Opt. Soc. Am. **58**, 63 (1968).
10. A. A. Friesem and U. Levy, Opt. Lett. **2**, 133 (1978).
11. B. Adams, "An Electro-Optic Imaging System Using Wavelength Coding," M.S.E.E. Thesis, U. Minnesota, Minneapolis (1981).
12. B. Adams and S. K. Case, Appl. Opt. **22**, 2026 (1983).
13. A. M. Tai and A. A. Friesem, Opt. Lett. **8**, 57 (1983).
14. D. E. Hulsey, "A Fiber Optic Imaging System using Wavelength Coding," M.S.E.E. Thesis, U. Minnesota, Minneapolis (1982).
15. S. K. Case, H. Bartelt, C. Henze, and D. Hulsey, in *Technical Digest, Topical Meeting on Optical Fiber Communication* (Optical Society of America, Washington, D.C., 1983), paper TUH6.

Polychromatic laser light source

C. P. Henze and S. K. Case

University of Minnesota, Electrical Engineering Department, Minneapolis, Minnesota 55455

(Received 9 May 1983; accepted for publication 18 May 1983)

We show that a commercial dye laser can be modified to allow rapid wavelength tuning via an applied voltage. By controlling the laser with a minicomputer, an arbitrarily specified continuous or discrete spectral output can be obtained.

PACS numbers: 42.60.By, 42.55.Mv

INTRODUCTION

A "white laser" would be useful for applications requiring a high-brightness polychromatic source. Such applications include polychromatic optical information processing[1] or the focusing of light into optical fibers for use with endoscopic imaging systems. In addition, such a source would be even more useful if its spectral output could be arbitrarily prescribed to achieve, for instance, a given color balance. In this paper, a method of producing such a high-brightness polychromatic light source by rapidly scanning a tunable dye laser through its spectrum with a computer generated periodic electronic control signal is described.

Most commercial tunable dye lasers have a birefringent crystal located within the laser cavity. This birefringent crystal is rotated mechanically to select the desired output wavelength. Such a mechanical tuning method is inherently slow. In our system, wavelength tuning is achieved electronically by placing a KD*P crystal which has a voltage-dependent birefringence into the optical cavity of a dye laser. A time-varying voltage applied to the crystal produces the wavelength scan so that rapid spectral scanning speeds are possible. If the dye laser is cycled through its spectral range at a rate at least equal to the frame rate of an integration detector such as the eye, a TV camera, or a photodiode array, the light will appear to have a continuous, distributed spectral output. By electronically varying the dwell time at various drive voltages (and hence wavelengths) within one spectral scan, the spectrum can be weighted so that a high-brightness polychromatic light source with arbitrary spectral output is produced. This source has both the focal and directional properties of a polychromatic laser when used with integrating detectors.

I. WAVELENGTH CONTROL

By incorporating an electronically tunable birefringent crystal into the optical cavity of a dye laser, the lasing wavelength may be controlled by a voltage applied across the crystal. This birefringent crystal has the property, such that, a multispectral beam incident upon the birefringent crystal would emerge spectrally redistributed in a conelike output beam. The angle that the constituent wavelengths would be rotated through when emerging from the birefringent crystal is a function of the electric field intensity within the crystal and hence a function of the voltage across the crystal. By applying the proper voltage, any desired wavelength can be made to propagate undeviated through the crystal to allow lasing. The crystal may be mechanically adjusted (rotated) to provide several tuning rates (nm/kV). These various tuning rates correspond to high-transmittance paths through the birefringent crystal with differing degrees of spectral dispersion.

A Spectra Physics model 375 dye laser with rhodamine chloride (R6G) dye and an argon ion pump laser is used. The dye laser is modified to allow the placement of the birefringent crystal[2] into the optical cavity as shown in Fig. 1. It was found necessary to realign the dye-laser mirror system to accommodate the path changes introduced by the insertion of the crystal. The crystal is mechanically adjusted such that an applied voltage from 0 to 2000 V will drive the dye-laser output through its full spectrum from 575 nm in the yellow–green to 635 nm in the red. By a suitable crystal reorientation and inversion of the applied voltage, the laser could be made to scan in the reverse direction through its spectrum. With a single fixed voltage applied to the crystal, a linewidth of 0.6 nm was measured.

Once the birefringent crystal is properly aligned, a digital computer is used in conjunction with a high-voltage operational amplifier to select the laser wavelength. The high-voltage operational amplifier is a current-to-voltage transresistance amplifier. The input current to the operational amplifier is provided by a software controlled digital-to-analog converter in a DEC LSI-11 computer. The digital-to-analog converter produces an output voltage

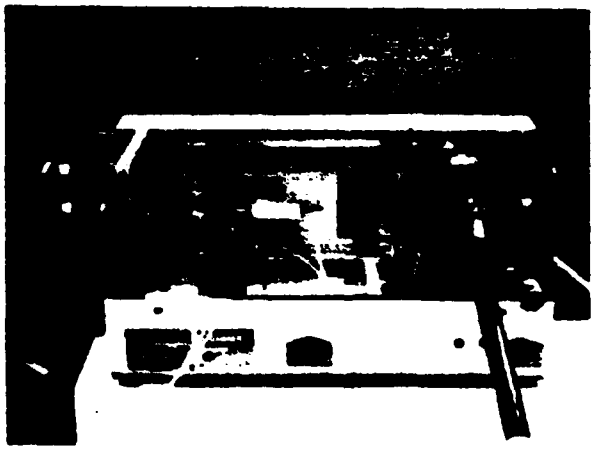

FIG. 1. KD*P crystal mounted inside dye-laser cavity.

 0034-6748/83/101334-04$01.30

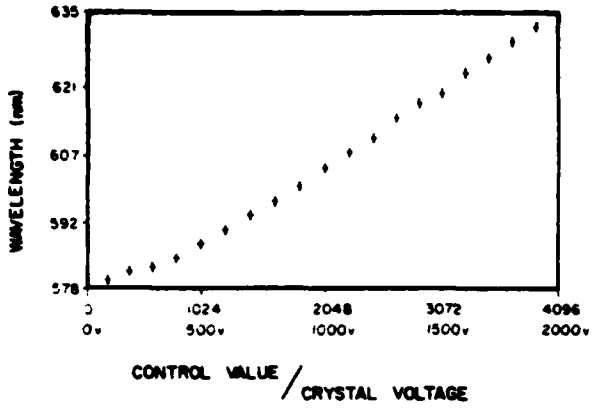

FIG. 2. Dye-laser wavelength vs the integer value loaded into the D/A converter.

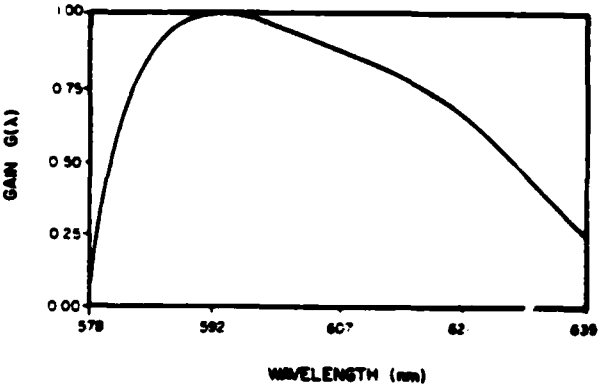

FIG. 3. Gain curve as a function of wavelength λ for the dye laser

(proportional to the value of a 12-bit input word) that ranges from 0.0 to 10.0 V corresponding to a 0.0–1.0-mA current drive to the amplifier.

Arbitrary periodic spectral distributions can be produced by sending digital values from a serial data string in computer memory, in the form of an endless loop, to the high-voltage operational amplifier through the D/A converter. The repetition period for the spectral scan is linearly proportional to the number of elements in the computer output string. The numerical (integer) value of a string element corresponds linearly to a unique wavelength λ between 575 and 635 nm as can be seen in Fig. 2.

As an example of our computer control routine, if it were desired to produce an output spectra which had only two discrete wavelengths located at the extreme values of 575 and 635 nm, one could load the first half of the string with the integer value "0" and the second half of the string with the integer value "4095" (the maximum value that can be expressed with 12 bits). The high-voltage operational amplifier would then drive the birefringent crystal with a maximum amplitude square wave, forcing the laser to spend half of its time at 575 nm and the other half at 635 nm. Corrections for the dye-laser gain and wavelength-dependent system losses could be achieved by varying the relative amount of 0's and 4095's in the computer output string to produce a nearly equal average intensity output for the two wavelengths.

II. GAIN CURVE MEASUREMENT

The output intensity of the light from the dye laser varies by an order of magnitude over the useful band of wavelengths. If it is desired to produce arbitrary spectra from the scanning dye-laser system described here, the natural gain curve of the system must first be measured and then be corrected for.

A measurement of the gain curve can be made by several methods. Discrete points may be measured and plotted or the entire curve may be displayed at once by scanning the laser wavelength linearly in time and passing the output light through a diffraction grating followed by a photodiode array. An important aspect of the scheme used to measure the gain curve is the further requirement needed to enter the data into the computer. If the gain curve is expected to vary as a result of pump laser output or other environmental changes, the curve measurement and normalization procedure should be fast enough to allow for frequent, rapid applications.

A numerical curve interpolation method is used in our interactive program, to measure, plot, and normalize the natural gain curve of the scanning dye-laser system. The output wavelength of the dye laser is set to a predetermined value by the computer. The output power is measured at that wavelength and entered into the computer. The output wavelength is then incremented by the computer to allow for the next measurement. Using the output power values and Newton's forward difference method[3] of curve interpolation the approximate power versus wavelength relationship (gain curve) is determined and plotted. It has been found experimentally that six measurements of the output power, each equally spaced in wavelength, provide sufficient information from which to reconstruct the gain curve. From six measurements a fifth-order polynomial is constructed which approximates the gain curve for the wavelengths of interest. An example of an interpolated gain curve is shown in Fig. 3 where the maximum gain has been normalized to unity.

Once the relative intensity of the output light is known as a function of wavelength, it is possible to determine the electronic wave shape that, when applied to the birefringent

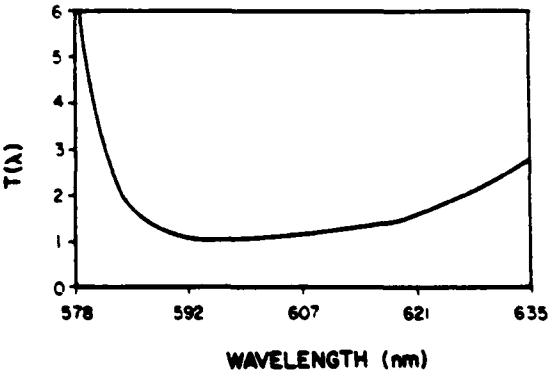

FIG. 4. Relative dwell time $T(\lambda)$ spent at each wavelength λ in order to achieve equal average intensity per unit wavelength across the spectrum.

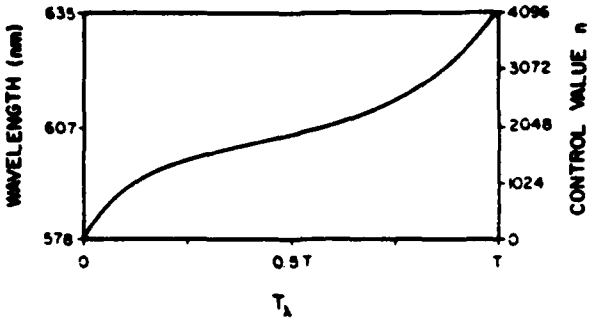

FIG. 5. Total elapsed time T_λ between beginning of cycle and the time the wavelength λ should be outputted.

crystal, will produce a desired spectral output. When scanning the dye laser through its spectrum with a periodic control voltage the average intensity at a given wavelength can be altered by changing the relative amount of time that the wavelength is present.

As one experiment, it was decided to produce an output that had constant intensity per unit wavelength across the spectrum since such a source does not otherwise exist in nature and may be useful for some experiments. To achieve this, it is required to spend more time at wavelengths where the output intensity is low. For a typical gain curve that is peaked in the center and falls off at the ends, a plot of the control voltage versus time must be "flatter" at both the beginning and the end of its cycle and "steeper" during the middle of its cycle in order to produce a constant intensity output over the spectral range. This suggests that a sinusoidal-type control voltage will produce a more spectrally flat output than would a linear sawtooth-type control voltage. The exact algorithm used to normalize the system gain curve, thus producing a constant amplitude spectrum, is described below.

The fitted gain curve $G(\lambda)$ is shown in Fig. 3. In order to produce a spectrum with equal average intensity per unit wavelength, the relative amount of time that must be spent at a given wavelength is

$$T(\lambda) = 1/G(\lambda), \tag{1}$$

as shown in Fig. 4. The total time T for one cycle is given by the integral of Eq. (1)

$$T = \int_{\lambda_{\min}}^{\lambda_{\max}} T(\lambda)\,d\lambda. \tag{2}$$

Similarly, the total time that has elapsed from the beginning of the scan until the wavelength λ is outputted given by

$$T_\lambda = \int_{\lambda_{\min}}^{\lambda} T(\lambda)\,d\lambda. \tag{3}$$

The result from Eq. (3) is shown in Fig. 5, where we have interchanged the axis and display elasped time horizontally and wavelength vertically. Figure 5 thus shows the waveshape we should produce at each particular time in order to achieve a flat spectrum. To incorporate the results of Fig. 5 into our computer program, we proceed as follows: The period was set at $T = 1/60$ s so as to be easily synchronized with a TV camera, which is the integrating detector often used in

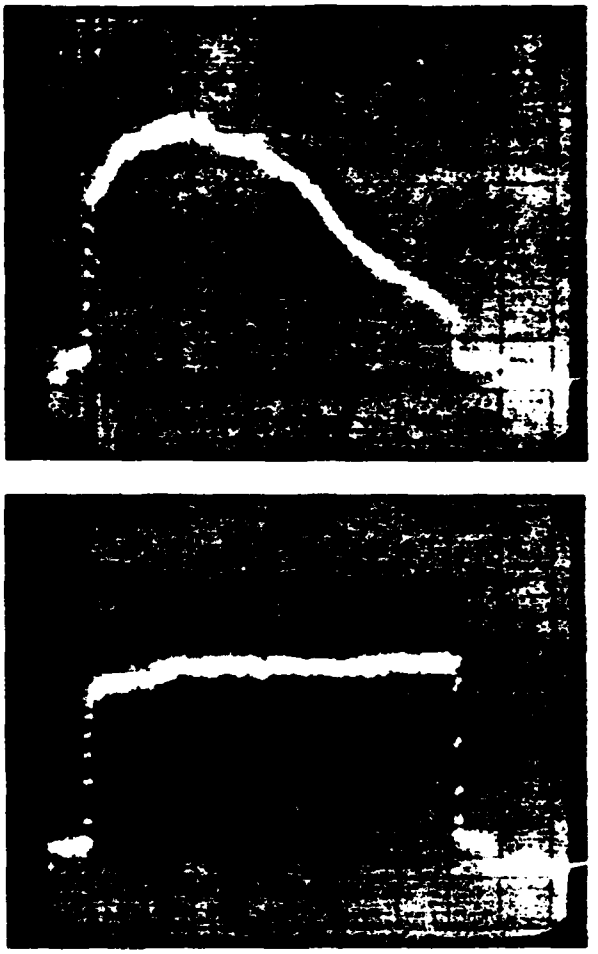

FIG. 6. (a) Natural spectral output of the dye-laser system observed on a photodiode array. (b) Spectral output after application of normalization routine.

our experiments. The drive voltage from our computer system can only be updated at $\Delta T = 73\ \mu$s intervals, so the horizontal axis in Fig. 5 is broken into $T/\Delta T = 192$ intervals. As shown in Fig. 3, the output wavelength is linearly related to the integer value n (between 0 and 4095) loaded

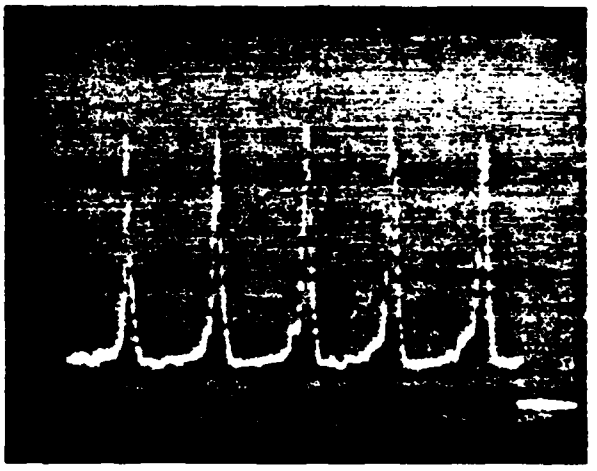

FIG. 7. Spectrum incorporating five equally spaced, equal average intensity wavelength peaks.

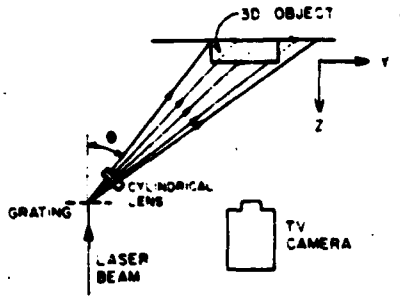

FIG. 8. Use of a computer-controlled dye laser for 3D robotic vision without moving parts.

into the D/A converter. The values n are shown on the right side of Fig. 5. From Fig. 5, therefore, we have the integer value n that must be loaded into the D/A converter for each of the 192 sequential times in one wavelength scan.

The 192 discrete voltage jumps produce a 14-kHz square wave that is superimposed upon the input to the high-voltage operational amplifier. However, the high-frequency response of the amplifier begins to roll off at 500 Hz. Therefore, the 14-kHz component does not appear in the voltage applied to the birefringent crystal. To lower the bandwidth requirements on the high-voltage amplifier, it is often advantageous to ramp the voltage up during one cycle and then ramp it down during the next cycle producing a triangle- rather than sawtooth-type waveform.

III. EXPERIMENTAL RESULTS

The results of our efforts to produce a flat output spectrum are shown in Fig. 6. The output beam from the laser is passed through a diffraction grating and the dispersed beam is focused onto a linear photodiode array. The "start of integration" signal from the self-scanned array is used to start the computer scan cycle so as to synchronize the laser and detector allowing the laser to make only one pass along the array before it is read out. In Fig. 6(a), the natural gain curve for the dye laser is obtained by driving each wavelength for an equal time. Deviations between Figs. 3 and 6(a) stem from the wavelength-dependent response of the detector array. In Fig. 6(b), the laser is scanned with weighted dwell times as previously described. As can be seen, the laser has a uniform output over its whole spectrum.

In Fig. 7, we show another pattern in which the laser produces five discrete wavelengths of nearly equal intensity and at equal wavelength intervals. The slight asymmetry seen near the base of each wavelength spike is due to the limited frequency response of the high-voltage amplifier. Of course the wavelength steps could be arbitrarily specified. One use for such a source is shown in Fig. 8. Here an adaptation of a 3D robotic vision scheme is shown. In the standard

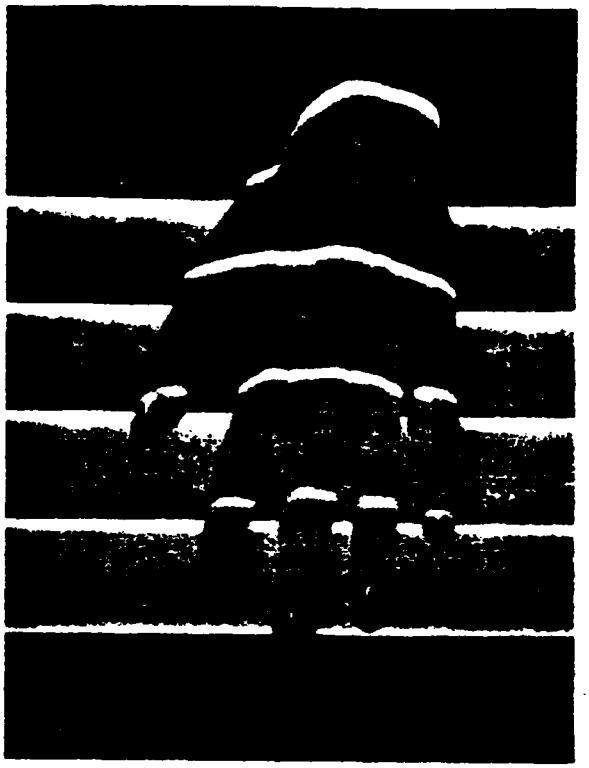

FIG. 9. Experimental results using the setup in Fig. 8. Each band of light is a different wavelength.

"light stripe" vision technique,[4] a sheet of light, obtained by expanding a laser beam with a cylindrical lens, is cast onto an object at an angle θ. By viewing the intersection of the sheet of light with the object, one can use triangulation to compute the object height z. To observe various positions y along the object, the beam is traditionally scanned in angle θ by a rotating mirror. In our scheme (Fig. 8), no moving parts are required. The polyspectral laser output (Fig. 7) is dispersed by a grating to produce a set of sheets of light. These intersect the object to give depth information as shown in Fig. 9.

ACKNOWLEDGMENTS

The authors thank the Army Research Office and the Air Force Office of Scientific Research (Grant DAAG 29-81-K-0033) for supporting this research.

[1] F. T. S. Yu and M. S. Dymek, Appl. Opt. 20, 1450 (1981).
[2] Ithaca Research Corporation, Model LS-14K-2, Electro-Scan Tuner.
[3] L. W. Johnson and R. D. Riess, Numerical Analysis, Addison-Wesley, Reading, MA, 1977, pp. 182–184.
[4] R. A. Jarvis, IEEE Trans. Pattern Anal. Mach. Intelligence, PAMI-5, 122 (1983).

1.4 Selected papers

Multifacet holographic optical elements for wavefront transformations.

Coordinate transformations via multifacet holographic optical elements.

Reprinted from Applied Optics, Vol. 20, August 1, 1981.

Multifacet holographic optical elements for wave front transformations

S. K. Case, P. R. Haugen, and O. J. Løkberg

A new type of holographic optical element combines some of the flexibility of computer-generated holograms with the high light efficiency of volume phase holograms to produce optical elements capable of arbitrary illumination transformations with nearly 100% light efficiency. The optical element is recorded by subdividing a volume hologram film surface into numerous small areas (facets), each of which is individually exposed. A final optical system consisting of two dichromated gelatin holograms in series is demonstrated. The first hologram spatially redistributes the incident light, and the second hologram produces a desired phase front on the redistributed light.

I. Introduction

It is often necessary to expand and spatially redistribute a beam of laser light prior to its use in a coherent optical system. Frequently one wishes to provide uniform object illumination or, alternately, to illuminate only specific areas on an object. The various expansion and redistribution methods in use[1-6] vary greatly in ease of implementation and optical efficiency, with these two attributes often not simultaneously present.

In this paper we demonstrate a new type of holographic optical element with which a coherent beam of light can be readily transformed to provide arbitrary illumination at arbitrarily prescribed spatial locations. The method utilizes nearly all the energy in a Gaussian input beam and produces an output beam with a smooth phase front.

II. New Optical System

We wish to coherently illuminate the edge of the hollow box in Fig. 1. Starting with a Gaussian intensity profile laser beam, a simple expansion of the beam, as in Fig. 1, would prove to be very light inefficient in that the intense center of the beam would fall into the hollow center of the box. If the walls of the box are thin compared to its lateral dimensions (a sparse object), only a very small fraction of the incident light would provide useful illumination (see the Appendix). A much more efficient illumination method for such an object would be to employ an optical system that would redistribute nearly all the laser light onto the periphery of the box. Our system for doing this is shown in Fig. 2 and employs two holographic optical elements in tandem. The first hologram acts to spatially redistribute the input light beam, and the second hologram produces a desired phase front on the redistributed light so that it can propagate toward a distant object.

A. Hologram #1 Design

Hologram #1 must efficiently diffract the light in an input beam such that the diffracted light has the desired spatial and intensity distribution when it reaches the plane of hologram #2. We could consider computer generation, interferometric generation, or generation of the hologram by a hybrid technique[7-12] as described in this paper. Computer generation would allow great redistribution flexibility but optical efficiency limited to ~40%.[13] A conventional volume phase hologram, on the other hand, could have nearly 100% diffraction efficiency but would offer limited flexibility in that it must be interferometrically recorded.[14]

The hybrid hologram described in this paper combines the best features of the previous hologram types: flexibility and high efficiency. Its design principle is straightforward. While the interference pattern required to interferometrically record an entire redistribution hologram is quite complex, the required pattern within any small area on the hologram is relatively simple such that it can be produced by the interference of a pair of plane waves. Thus, our solution is to produce a multifacet hologram which is recorded by subdividing a volume hologram film surface into numerous

The authors are with University of Minnesota, Electrical Engineering Department, Minneapolis, Minnesota 55455.
Received 22 April 1981.
0003-6935/81/152670-06$00/0.

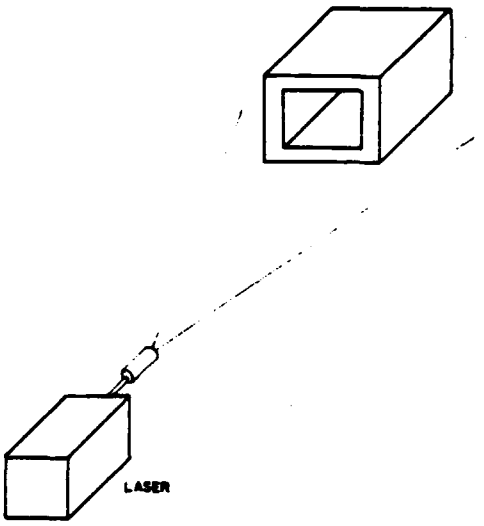

Fig. 1. Inefficient method for illuminating the periphery of a large hollow box.

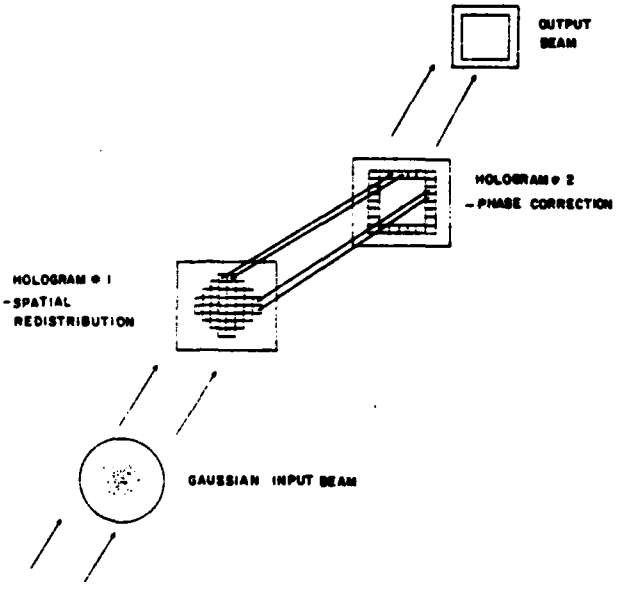

Fig. 2. Wave front transformation system for efficient illumination of the object.

small cells (facets), each of which is individually exposed. Each facet contains a plane wave grating which diffracts the light from a given location in the input beam to the proper output location. By constructing the hologram in a volume phase material, such as dichromated gelatin, each facet can achieve nearly 100% diffraction efficiency into a single diffracted order.

The design of our optical element starts by assuming that the input beam will have a Gaussian irradiance profile. This input light distribution is shown in Fig. 3(a), where we have divided the Gaussian beam into forty-four cells and calculated the relative irradiance in each cell. All light out to the radius where the irradiance falls to $1/e^2$ of its peak value will be used in the redistribution. The light in the cells of Fig. 3(a) becomes the building blocks for the desired output pattern. By spatially redistributing the light in these cells, we can arrive at the desired box-shaped output distribution given by the top numbers in the cells in Fig. 3(b). We note, for example, that the light from the center of the Gaussian distribution will be mapped to the corners of the box. We also note that the forty-four input cells will be mapped to twenty-four output cells to achieve an output intensity distribution which varies by less than a factor of 2 (1*f*/stop). That is, the light from more than one input cell will often be mapped to a given output location. This particular intensity smoothing operation works well for some systems but will cause problems with others, as will be described later.

B. Hologram #1 Recording

The individual facets in the hologram are serially constructed using the holographic setup shown in Fig. 4. The holographic film is held on a computer-controlled translation stage which is advanced by one facet width between each exposure. A thin stationary flexible mask containing an aperture used to select the facet shape and size is pressed lightly against the film. This geometry allows good construction beam overlap

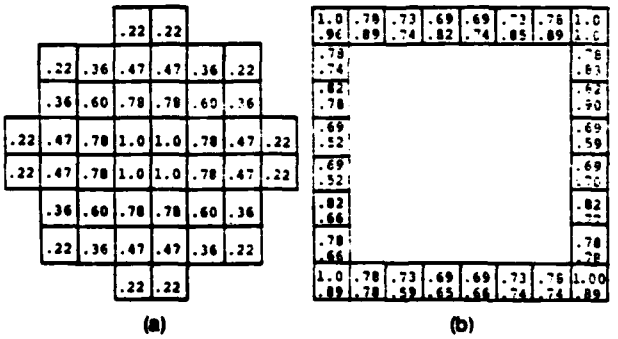

Fig. 3. Irradiance distributions: (a) input beam and (b) output beam.

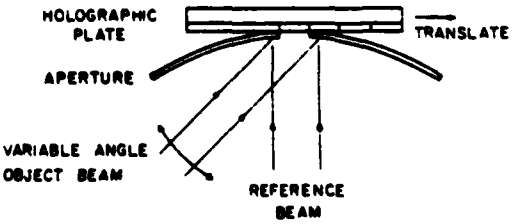

Fig. 4. Setup for recording multifacet holograms.

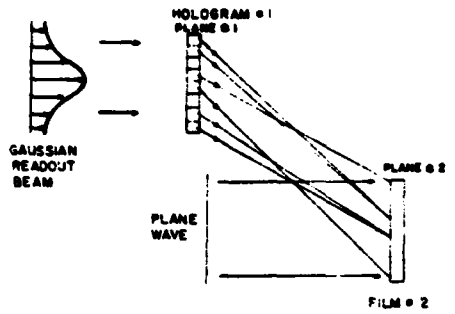

Fig. 5. Top view of optical system showing redistributed light from hologram #1 being used as the object wave to record hologram #2.

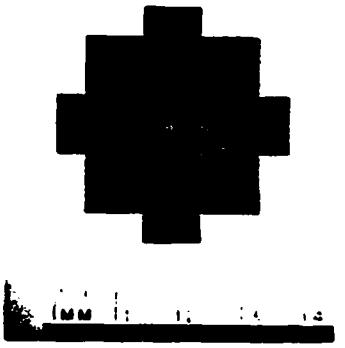

Fig. 6. Multifacet hologram recorded in absorption material (for illustration). Volume phase holograms were used for all experiments.

and minimizes aperture diffraction effects or shadowing. The aperture mask allows one facet to be recorded at one time.

The grating within each facet is recorded by exposure with two coherent plane waves. The reference wave is incident normal to the film and is at the same angle for each facet. The object wave is incident at ~30° with respect to the film normal, with the exact incidence angle selected by reflecting the object beam from a pivotable mirror. The object beam angle for a given facet is merely set at the required angle, which will map the input light from a given location on hologram #1 to the desired output location in plane #2.

The holograms are recorded in dichromated gelatin at a wavelength $\lambda = 0.488\ \mu m$. The gelatin layer is obtained from Kodak 649-F plates by processing instructions given in Ref. 15. These are similar to those of Chang and Leonard.[16] A diffraction efficiency vs exposure curve for the film is given in Refs. 10 and 15. For an exposure of ~80 mJ/cm^2, the gratings have nearly 100% diffraction efficiency (ignoring surface reflections) so that all the incident light is diffracted toward the desired output.

After exposure of all the facets, and development, the hologram is illuminated with the expanded Gaussian input beam, as in the top view in Fig. 5. The Gaussian beam has a planar wave front and is normally incident on the hologram so that the Bragg condition for each facet is satisfied. The diffracted light propagates from the hologram and is spatially redistributed upon arrival at plane #2.

In addition to redistribution flexibility there are several advantages to constructing the hologram via a multifacet approach. First, the recording beams are plane waves, which are easy to produce. Because the individual facets to be recorded are small, the recording beams can be of small diameter, which leads to high exposure beam irradiance and short exposure times. In addition, one can ensure unity object beam/reference beam irradiance ratios and optimum exposure at each location on the hologram for maximum diffraction efficiency. Also, with plane wave recording one can specify both the spatial frequency and the Bragg angles of the grating within each facet so that arbitrary spatial redistribution and maximum diffraction efficiency are simultaneously possible. It is even possible to adjust the recording waves to produce holograms with the proper spatial frequency and Bragg angles to enact high efficiency redistribution when read out at a wavelength (e.g., $\lambda = 6328$ Å or $1.06\ \mu m$) for which efficient recording films are not sensitive.[17]

C. Hologram #2

As shown in Fig. 5, the light arrives at plane #2 from many different angles. If our object can be located at plane #2, and we are only interested in the intensity at the object surface, no second hologram is required. However, it is often desirable or necessary to be able to illuminate a more distant object, to scale the illumination beam (for different size objects), or to illuminate the object from only one direction (for interferometry). For these purposes we require the spatially redistributed light to have a smooth phase front. Such a phase front can easily be produced by the use of a second hologram. The recording of a typical second hologram is illustrated in Fig. 5. Here, the spatially redistributed light arriving from hologram #1 and a planar reference wave coherently expose film #2. After development and exact replacement of the second hologram, the hologram pair can be used as shown in Fig. 2 to produce the square output beam, which, because of its flat phase front, will propagate toward a distant object. Slow beam degradation, of course, will result from Fresnel diffraction.

III. Experimental Results

Hologram #1 contains forty-four facets, each of which is ~5 × 5 mm in size. The holograms were recorded in dichromated gelatin film as described earlier. Because it is difficult to photograph phase holograms, Fig. 6 shows a replica of hologram #1 recorded in Kodak 649-F.

As the light leaves the first hologram and propagates toward plane #2, the spatial light distribution changes from the near circular pattern to the square one. The gradual redistribution is shown in Fig. 7. Here the light distribution was photographed in five equally spaced planes to make the composite picture.

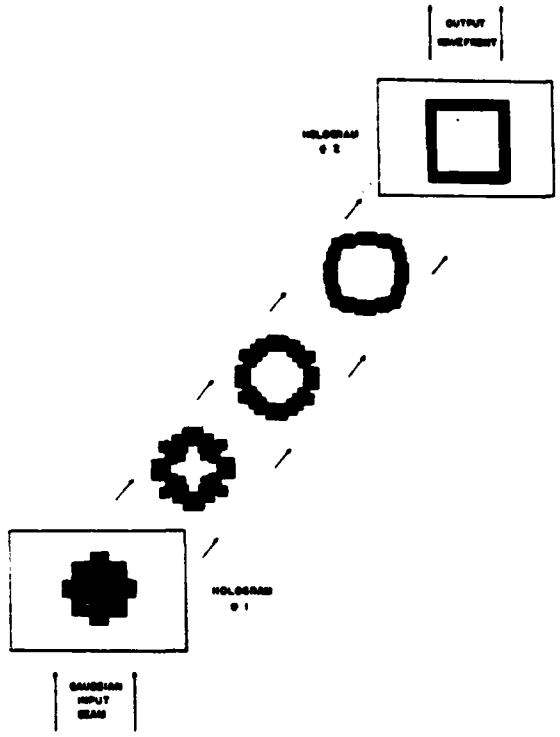

Fig. 7. Redistribution of light between input and output planes.

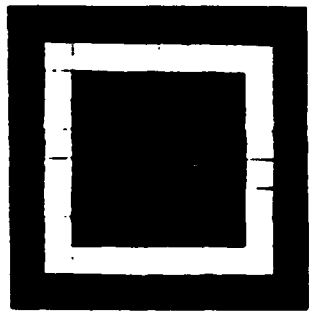

Fig. 8. Output light distribution.

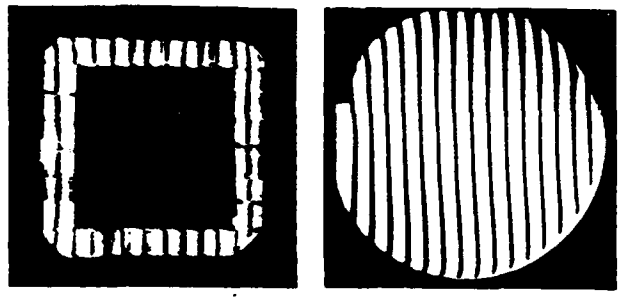

(a) (b)

Fig. 9. Interferograms showing wave front quality: (a) output wave and (b) reference wave.

Plane #2 was located ~25 cm after plane #1. This distance was chosen as a compromise so that neither the range of deflection angles required from hologram #1 nor the effects of Fresnel diffraction from the individual facets would be excessively large. A photograph of the light distribution in plane #2 is shown in Fig. 8. Manual object beam steering was used to produce hologram #1 in this case and resulted in the small gaps between output cells. Steering for hologram recording is now done under computer control. The measured intensity distribution in plane #2 is shown as the lower number in each cell of Fig. 3(b). The intensities are normalized to compensate for surface reflection losses and allow easy comparison with the theoretical values (upper number in each cell). It is seen that the design goal of <50% output intensity variation has been met. Due to the nonperfect Gaussian readout beam, some cells are seen to have slightly greater than the predicted intensity.

As stated earlier, if our only concern is with output intensity no second hologram is required. To achieve a flat phase front on the output beam, however, we have employed a second dichromated gelatin hologram. In Fig. 9(a) we show an interferogram of the output wave front 50 cm after hologram #2. The straight fringes attest to the wave front quality. The square shape has also been retained after the 50-cm propagation. The rounding of the corners is due to finite sized interferometer optics. Figure 9(b) shows an interferogram of the plane wave used to record the second hologram (for reference).

If wave front phase correction (via the second hologram) is desired, the simple intensity smoothing operation, consisting of mapping the light from several cells in plane #1 to one output cell in plane #2, should be avoided. This is because intermodulation in the second hologram will result in the production of several diffracted output waves instead of just one desired output wave. Other intensity smoothing schemes such as using object beams with variable focal power could be used. Of course, if phase correction of the output light is not needed, the simple multiple mapping technique works very well.

IV. Conclusion

We have demonstrated a technique whereby an input light distribution can be mapped to an arbitrarily prescribed output light distribution. The technique employs two holograms in which the first hologram enacts the spatial redistribution of light and the second hologram produces a desired (e.g., diverging, collimated, or converging) wave front on the output light. Digital control of the interferometric recording process allows precise production of custom optical elements. The use of volume phase holograms for the redistribution process leads to high optical efficiency.

To provide illumination to specific locations on an object, the light intensity obtained via our redistribution method is much greater than that obtained by simply expanding an incident laser beam, as is shown in the calculations in the Appendix. Although we have shown

one use of multifacet holograms in this paper, such holograms can find additional use for space variant optical processing, customized holographic optical elements, coding and decoding elements, pseudocoloring, and optical computing.

The authors thank the Research Corporation (grant #9000) and the University of Minnesota for the support of this research.

O. J. Løkberg is on leave from Norwegian Institute of Technology, Physics Department, N-7034 Trondheim, Norway.

Appendix

We calculate the light efficiency gain obtained by using our custom redistribution hologram to redistribute most of the light in a Gaussian beam exactly onto the object, as opposed to simply expanding a Gaussian beam to provide object illumination.

We start with a Gaussian laser beam with amplitude

$$A(r) = A_0 \exp[-(r/\omega_0)^2]. \tag{A1}$$

For this calculation we assume that we want to optimally illuminate an annulus[18] with radius r_0 and width αr_0, as in Fig. 10. The circular symmetry of our subject was chosen to enable a simple mathematical solution to the problem. If the laser beam is expanded to have a new waist radius ω_1, it will have amplitude

$$A_1(r) = A_0 \frac{\omega_0}{\omega_1} \exp\left[-\left(\frac{r}{\omega_1}\right)^2\right]. \tag{A2}$$

We can show that the irradiance at radius r_0 is maximized if we expand the beam so that $\omega_1 = \sqrt{2} r_0$, which means that the beam is expanded to have an irradiance at radius r_0 equal to $1/e$ of its peak ($r = 0$) irradiance. Using this with Eq. (2) yields an irradiance

$$I_1(r) = \frac{A_0^2}{2}\left(\frac{\omega_0}{r_0}\right)^2 \exp\left[-\left(\frac{r}{r_0}\right)^2\right]. \tag{A3}$$

The total optical power falling on the annulus is then

$$P = \int_{r_{min}}^{r_{max}} I_1(r) 2\pi r dr, \tag{A4}$$

$$= \frac{\pi A_0^2 \omega_0^2}{2}\left\{\exp\left[-\left(\frac{r_{min}}{r_0}\right)^2\right] - \exp\left[-\left(\frac{r_{max}}{r_0}\right)^2\right]\right\}. \tag{A5}$$

Since the total power in the laser beam is

$$P_0 = \frac{\pi A_0^2 \omega_0^2}{2}, \tag{A6}$$

$$r_{min} = r_0\left(1 - \frac{\alpha}{2}\right), \qquad r_{max} = r_0\left(1 + \frac{\alpha}{2}\right), \tag{A7}$$

the fraction of total laser power used for illumination is

$$F = \frac{P}{P_0} = \left\{\exp\left[-\left(1 - \frac{\alpha}{2}\right)^2\right] - \exp\left[-\left(1 + \frac{\alpha}{2}\right)^2\right]\right\}. \tag{A8}$$

As stated earlier, our particular redistribution hologram utilizes the laser beam out to the radius where $I = I_{max}^2/\exp(2)$. The fraction of the beam power incident on our hologram is, therefore,

$$F' = [1 - \exp(-2)] = 86\%. \tag{A9}$$

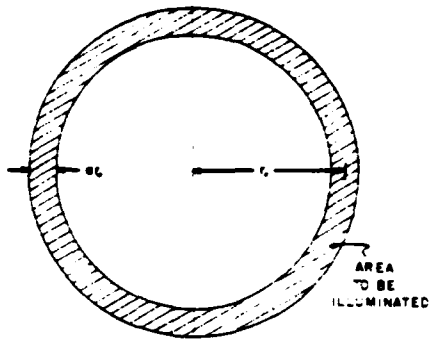

Fig. 10. General object to be illuminated.

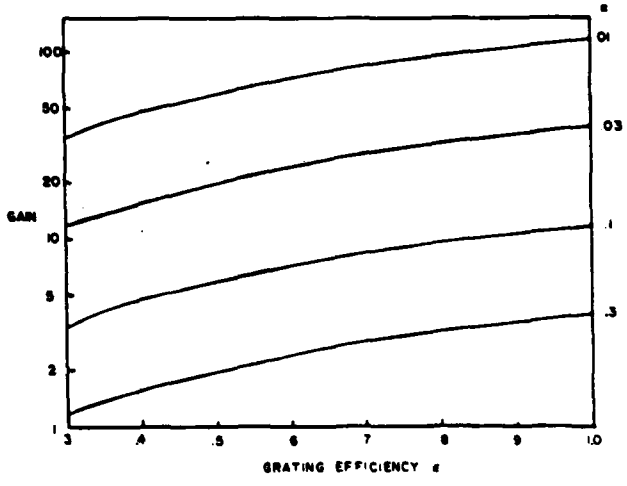

Fig. 11. Light gain when using one redistribution hologram.

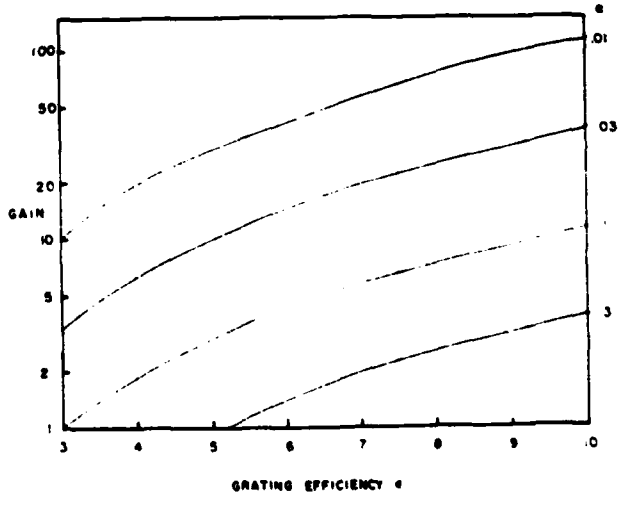

Fig. 12. Light gain when using two redistribution holograms.

If our hologram has diffraction efficiency ϵ, the fraction of light arriving at the redistributed plane is $F_1 = 0.86\epsilon$. The gain in light intensity with our new method is, therefore,

$$G_1 = F_1/F = 0.86\epsilon/F. \quad (10)$$

If a two-hologram redistribution system is used, the gain becomes

$$G_2 = 0.86\epsilon^2/F. \quad (11)$$

These two gains are plotted in Figs. 11 and 12 with α as a parameter. We see that for high efficiency holograms and sparse objects ($\alpha < 0.1$), the gain can be greater than a factor of 10.

References

1. M. Quintanilla and A. M. deFrutos, Appl. Opt. **20**, 879 (1981).
2. See segmented mirror from Spawr Optical Research, Inc., 1527 Pomona Rd., Corona, Calif. 91720. This method does not produce illumination with a smooth phase front.
3. P. W. Rhodes and D. L. Shealy, Appl. Opt. **19**, 3545 (1980).
4. Stencil Marker by Lumonics, Inc., 105 Schneider Rd., Kanata, Ontario, Canada K2K 1Y3.
5. N. C. Gallagher and D. W. Sweeney, IEEE J. Quantum Electron. **QE-15**, 1369 (1979).
6. D. W. Sweeney *et al.*, Appl. Opt. **15**, 2959 (1976).
7. A. multifacet volume hologram technique was first described by S. K. Case and V. Gerbig at the Deutsche Gesellschaft für Angewandte Optik annual meeting in Bad Harzburg, West Germany, June, 1979.
8. S. K. Case and V. Gerbig, Opt. Engineer. **19**, 711 (1980).
9. V. Gerbig, Opt. Commun. **36**, 90 (1981).
10. S. K. Case and V. Gerbig, Opt. Commun. **36**, 94 (1981).
11. U. Levy, A. A. Friesem, and B. Sharon, Appl. Opt. **19**, 1661 (1980).
12. The work in this paper was presented at the annual meeting of the Optical Society of America, 14–17 Oct. 1980, Chicago, Ill., J. Opt. Soc. Am. **70**, 1625A (1980).
13. B. R. Brown and A. W. Lohmann, IBM J. Res. Develop. **13**, 160 (1969).
14. Light reflected from an object could be used for one of the recording waves. This standard holographic technique could work if the object were available and small. For larger complicated objects, for which we may also desire arbitrary illumination intensities, this technique would not be easy to implement. One particularly limiting factor is that the high exposure levels required by efficient hologram materials such as dichromated gelatin coupled with the relatively weak light reflected from diffuse objects would mandate excessively long exposure times. The technique also would not work if $\lambda_{\text{recording}} \neq \lambda_{\text{readout}}$.
15. S. K. Case, *Multiple Exposure Holography in Volume Materials*, Ph.D. Thesis, U. Michigan, 1976 (Xerox University Microfilms order #76-27461).
16. B. J. Chang and C. D. Leonard, Appl. Opt. **18**, 2407 (1979).
17. S. K. Case and W. J. Dallas, Appl. Opt. **17**, 2537 (1978).
18. One could use an axicon to produce annular illumination; however, this is a special case where a conventional optical element could do our redistribution. We wish to treat the problem more generally.

Coordinate transformations via multifacet holographic optical elements

H. Bartelt
S. K. Case
University of Minnesota
Department of Electrical Engineering
123 Church Street S.E.
Minneapolis, Minnesota 55455

Abstract. Arbitrarily prescribed space variant operations can be carried out with high efficiency by multifacet holographic optical elements recorded in dichromated gelatin. In this paper, such elements are used to perform coordinate transformations from Cartesian to polar coordinates. Theoretical calculations of resolution limits and experimental results are given.

Keywords: holographic optical elements; space variant; optical computing.

Optical Engineering 22(4), 497-500 (July/August 1983).

CONTENTS

1. SPACE VARIANT OPERATIONS IN OPTICS

A coordinate transformation such as a transformation from Cartesian to polar coordinates represents a highly space variant operation. Most optical systems, however, are limited to space invariant processing. Very flexible optical components to generate more general transformations, especially for an arbitrary redistribution of light, can be achieved by using multifacet holographic optical elements (HOE).[1,2] These HOEs consist of many small and simple subholograms (e.g., holographic gratings) placed next to each other on a holographic plate. The subholograms are recorded under computer control, which allows great flexibility in the production of the HOEs. Each of the subholograms can change a portion of a large illuminating wavefront. The change can consist, for example, of the deflection or focusing of various portions of an incident plane wavefront. Since adjacent subholograms are independent of each other, space variant operations become possible with this type of HOE. In addition, dichromated gelatin is used as the recording material to achieve very high diffraction efficiency for the elements.[3] This method allows, therefore, a synthesis of operations with high light efficiency which is generally not possible by conventional optics.[4] We should mention that another approach to the problem of optical space variant operations by spatial filtering is described by Bryngdahl.[5] His method uses computer-generated gratings and a spatially modulated object.

2. MULTIFACET OPTICAL ELEMENTS

In this section, we describe the production of multifacet holographic optical elements. The fabrication begins by mentally subdividing the holographic plate surface into numerous small adjacent areas or facets. Each facet or subhologram is separately recorded by interfering relatively simple wavefronts such as plane or spherical waves. For simplicity, we will restrict ourselves in the following description to the case of plane waves.

Paper 1905 received Sept. 9, 1982; revised manuscript received Dec. 13, 1982; accepted for publication Jan. 11, 1983; received by Managing Editor Jan. 17, 1983.

In our setup, a flexible, stationary mask containing a small, square, open aperture contacts the holographic film to allow exposure of one facet at one time (see Fig. 1). Before recording, a prescribed area on the holographic plate is placed behind the mask opening via computer-controlled stepping stages. A mirror is also rotated under computer control so as to deflect the object wave at the appropriate angle for recording this facet. Exposure of the facet with the object wave and a plane reference wave (which is the same for each facet) occurs under computer control. This process is repeated sequentially until all subareas on the hologram have been exposed.

After development, all facets of the holographic plate are simultaneously illuminated by a large reference wave. The reconstruction of each subhologram produces a plane wave of small area with a prescribed output direction (see Fig. 2). A rearranged light distribution then appears in the near field behind the holographic plate. The light in this output plane consists of blocks or patches of light which originated from different spatial locations in the input plane (Fig. 2). An input transparency placed in contact with the hologram will be sampled by the hologram facets and have its pixel information spatially rearranged when it arrives at the output plane, thus producing, in our case, a coordinate transformation on the input information.

To achieve greatest accuracy in our transformations, the number of facets should be as large as possible. Since our holographic plate has finite size, we therefore endeavor to make the facets as small as possible. As the facets become smaller, however, Fresnel diffraction from the small aperture becomes increasingly problematic. Although our output plane is currently in the Fresnel region behind our hologram, further reduction of the facet size would place us in the Fraunhofer region, where it is easier to calculate achievable resolution and maximum sampling densities. Assuming Fraunhofer diffraction, a facet of size Δx_F gives a diffraction pattern at distance d of

$$f(x_R) = \Delta x_F \operatorname{sinc}\left(\frac{\Delta x_F\, x_R}{\lambda d}\right) , \tag{1}$$

where λ represents wavelength and x_R is the output plane coordinate. Decreasing the size of facets for high resolution in the hologram plane results therefore in a larger diffraction spot Δx_R in the output plane. Optimum resolution for both planes is assumed if the facet and diffraction spot are of equal size:

$$\Delta x_F = \Delta x_R = \frac{2\lambda d}{\Delta x_F} , \tag{2}$$

$$\Rightarrow \quad \Delta x_F = \sqrt{2\lambda d} . \tag{3}$$

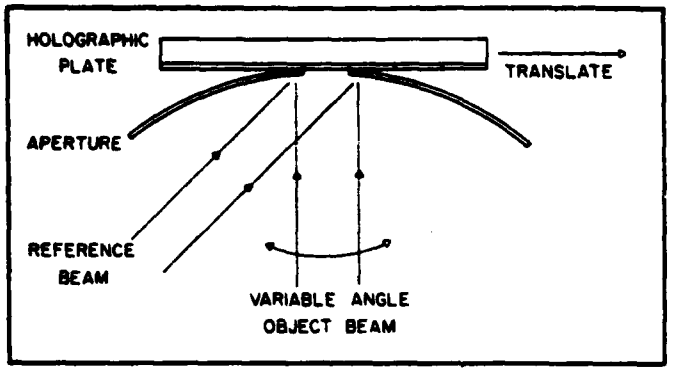

Fig. 1. Setup for recording multifacet holographic elements.

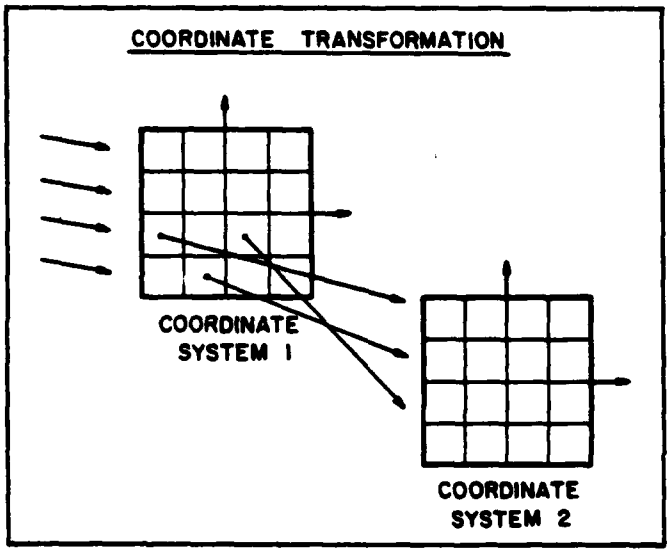

Fig. 2. Light redistribution by multifacet holographic elements.

A similar result can be obtained using a parageometrical analysis of Fresnel diffraction.[6] As an example [from (Eq. 3)], we get, for a reconstruction distance of d = 20 cm with λ = 488 nm, maximum resolution when $\Delta x_F = 0.44$ mm. To calculate the number of addressable pixels per line for an arbitrary redistribution, we must also consider the range of deflection angles $\Delta\alpha$, which is limited by practical considerations. With $\Delta\alpha = 45°$, we have the number of output pixels

$$N = \frac{d \tan\left(\frac{\Delta\alpha}{2}\right)}{\sqrt{2\lambda d}} \simeq 188 . \tag{4}$$

This assumes that each input facet must be able to address each output pixel position. This worst-case estimate yields as the possible number of facets approximately 200×200 and would require a hologram size of ~9×9 cm. For most redistributions, the spatial positions of the facets and the angular deflection required from them will be such that the total number of pixels can be larger. Of course, different geometries and different maximum deflection angles will change additionally the above estimates.

The basic holograms can also be modified to change the characteristics of the whole optical element. Introducing additional lenses such as spherical or cylindrical lenses in the recording beam allows one to alter the facet shape between the hologram and reconstruction planes. For instance, by using a cylindrical lens during recording, one can record facets whose output expands in one direction

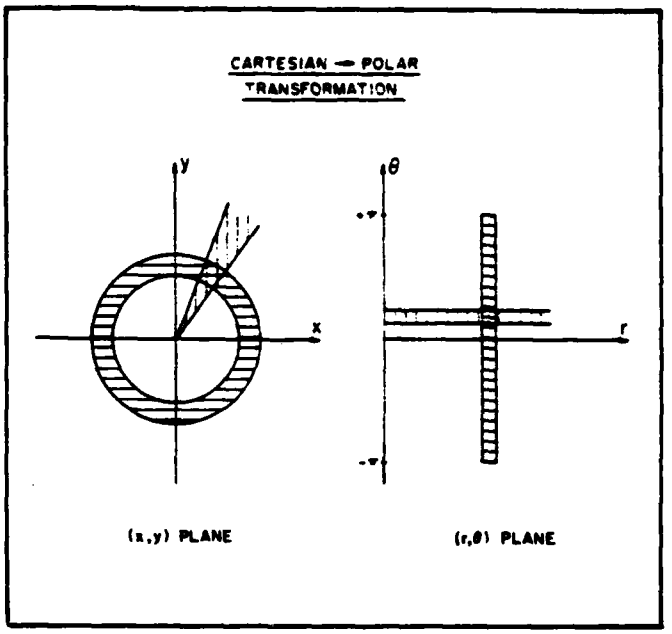

Fig. 3. Transformation from (x, y) coordinates to (r, θ) coordinates.

while propagating to the output plane. This is useful in some instances, as will be described later.

With the holographic elements discussed so far, phase is not controlled in the reconstruction plane. Light intensity distributions are therefore transformed. It is possible, however, to correct for output phase by use of a second hologram which is recorded in the reconstruction plane of the first hologram.[1]

3. CARTESIAN TO POLAR COORDINATE TRANSFORMATION

We will now turn to the specific application of multifacet optical elements for coordinate transformations. A coordinate transformation from Cartesian (x, y) to polar (r, θ) coordinates is described by

$$r = \sqrt{x^2 + y^2} ; \qquad \theta = \arctan y/x . \tag{5}$$

Rings in the (x, y) plane will be transformed into vertical lines in the (r, θ) plane, and circle segments (wedges) in the (x, y) plane into horizontal lines in the (r, θ) plane (Fig. 3). With this transformation, the size of elementary area elements varies with radius r. That is,

$$dxdy \neq rdrd\theta . \tag{6}$$

This means that, ideally, the light output from each facet in the (x, y) plane should be suitably stretched before arriving in the output plane. For our first coordinate transformation elements, however, we did not change the shape of the facets. As a first approach we built an element for transformation into a $(\sqrt{r}, \theta)$ plane, where no change in elementary area size occurs. In this case all rings to be transformed into one vertical line in the $(\sqrt{r}, \theta)$ plane cover the same surface area in the hologram plane. In Fig. 4 we show the output from the hologram for this transformation which contains 896 facets, each 1.7×1.7 mm in size. Successive annular zones, each containing 32 facets, are mapped into one vertical line in the output plane. For this reason, radial resolution is low for small radii, and fewer radii are resolved in comparison to the method described in the next paragraph. The output light has been photographed in several different planes between the hologram and output planes in order to show the gradual redistribution of light during the transformation.

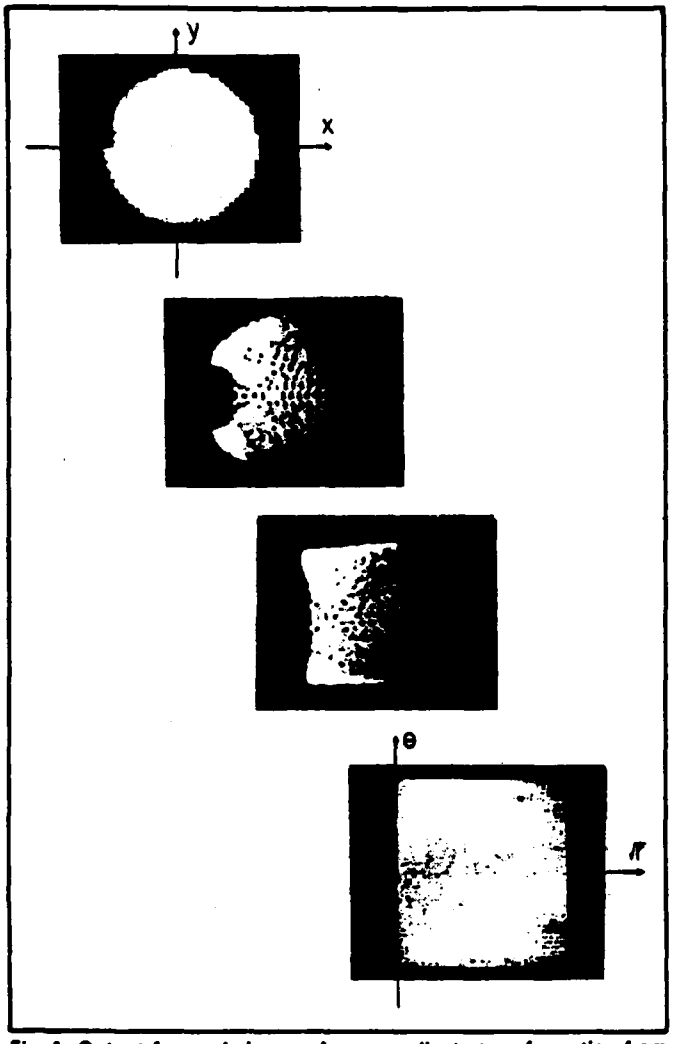

Fig. 4. Output from a hologram for a coordinate transformation from (x, y) coordinates into ($\sqrt{r}$, θ) coordinates in different planes between hologram and output plane.

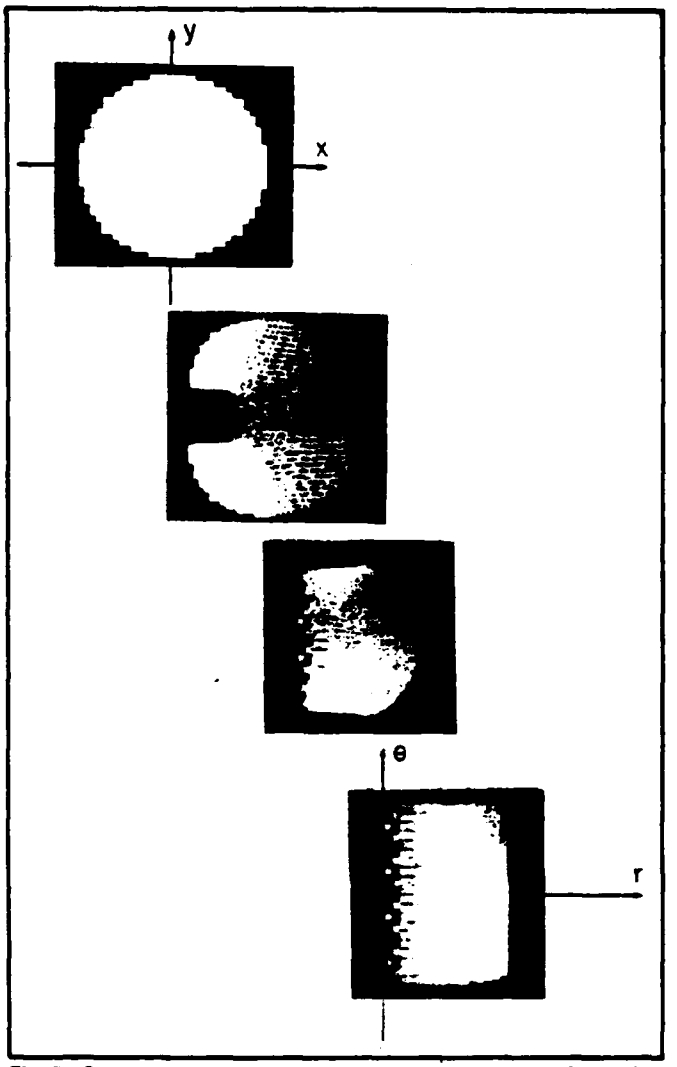

Fig. 5. Output from a hologram for a coordinate transformation from (x, y) coordinates into (r, θ) coordinates in different planes between hologram and output plane.

For a transformation into (r, θ) coordinates, rings of equal dr-width in the hologram plane are displayed as successive vertical lines in the output plane. In this hologram the facet outputs were not stretched, but were simply centered at the proper θ position for the facet in the output plane. Because of the fixed size of the facets, the output pixels occasionally overlap or show dark gaps in the (r, θ) plane. In Fig. 5 a flying light picture of an (x, y) → (r, θ) holographic element with 823 facets is shown.

It is possible to vary the shape of the output facets by introducing additional focal power in the hologram. Cylindrical lenses can be used to change the elementary plane waves into proper converging or diverging waves. In this manner overlapping or gaps in the output plane are removed and resolution and contrast are improved. Figure 6 demonstrates this effect for the first three vertical lines in the (r, θ) plane.

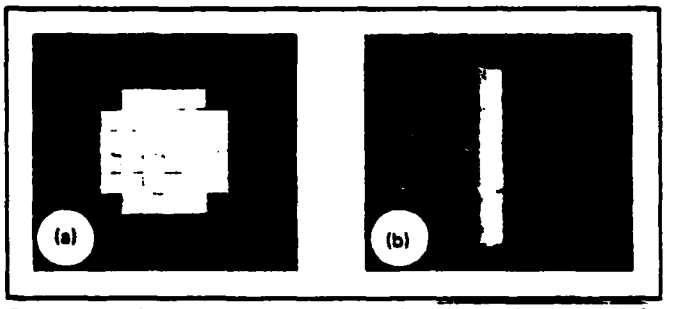

Fig. 6. Light from a hologram with varying shape of output pixels: (a) hologram plane (shown enlarged); (b) output plane.

4. EXPERIMENTAL RESULTS

In the following we will show some examples of transformations. Object transparencies were placed in contact with the holographic elements, which were about 55 mm in diameter. Argon laser illumination at λ = 488 nm was used. The holograms were recorded at the same wavelength in dichromated gelatin for high diffraction efficiency (>90%). The output plane is located a distance d = 200 mm after the hologram plane.

The holographic element shown in Fig. 4 was designed to resolve 8 different radii and 16 different angles. The element in Fig. 5 has a resolution of 16 radii and a varying resolution of angles between 4 and 24 depending on radius. In Figs. 7-11 the HOE from Fig. 5 was applied to different object patterns. In the figures the input transparency used is shown on the left and the resulting output light distribu-

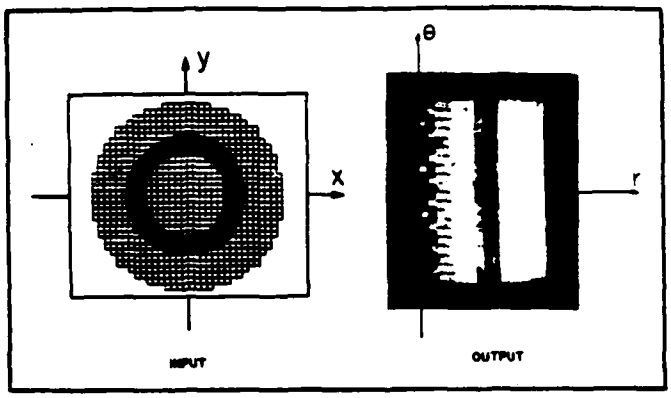

Fig. 7. Ring object and transformation.

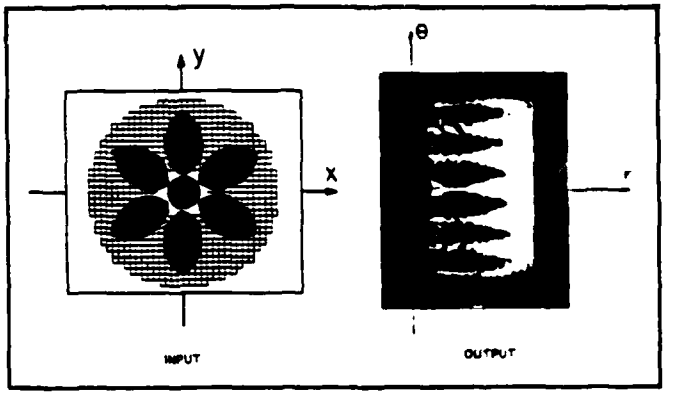

Fig. 10. Circular symmetric object and transformation.

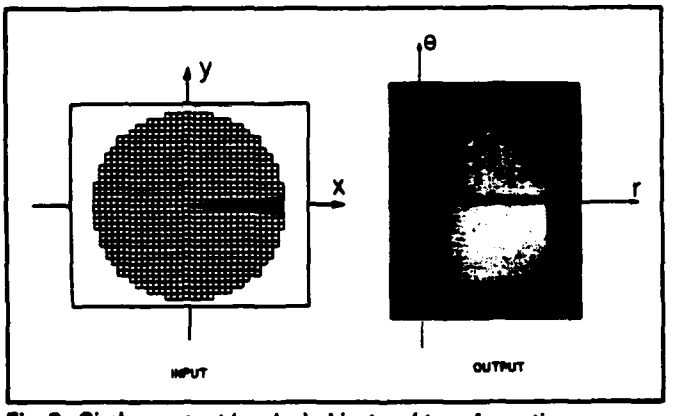

Fig. 8. Circle segment (wedge) object and transformation.

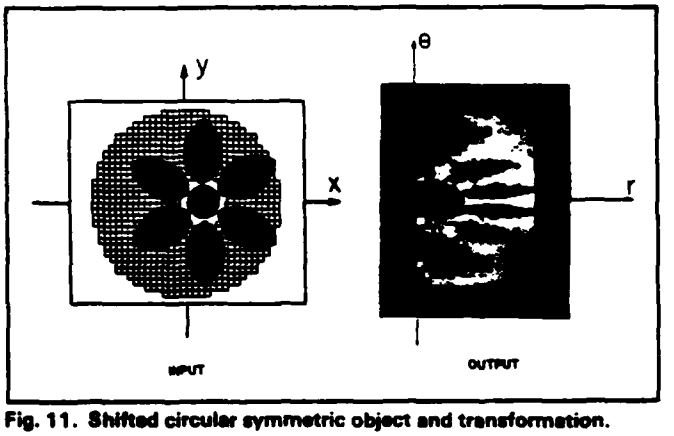

Fig. 11. Shifted circular symmetric object and transformation.

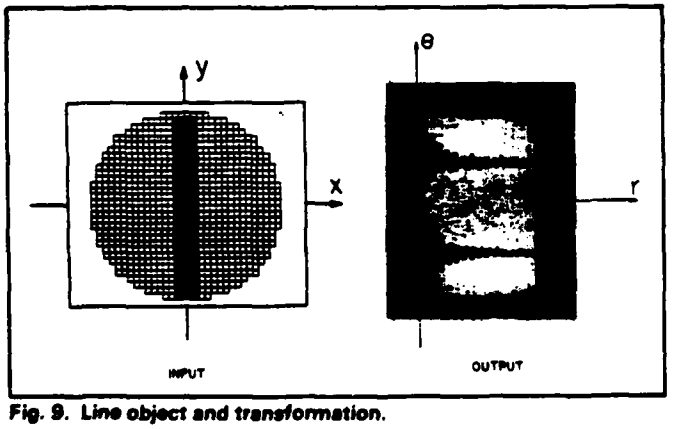

Fig. 9. Line object and transformation.

tion is shown on the right.

Figures 7 and 8 show how rings and circle segments (wedges) are converted into lines. The thick line input object in Fig. 9 results in two cone-shaped distributions in the (r, θ) plane due to the varying angular width of the object with radius. A center symmetric object was used in Fig. 10. Such transforms could be useful for rotation-invariant pattern recognition. A shift of the object results in the modified output shown in Fig. 11. It should be mentioned that gray-level pictures can be transformed in the same manner.

5. CONCLUSIONS

We have shown that multifacet optical elements can be used to perform space variant operations such as coordinate transformations. They combine high flexibility with high light efficiency when recorded in dichromated gelatin. The transformation from Cartesian to polar coordinates can be applied for detection of circular symmetric objects or for centering parts. In general, with multifacet optical elements other types of coordinate transformations or optical mappings can be implemented.

6. ACKNOWLEDGMENTS

The authors thank P. R. Haugen for assistance with the optical setup and computer interfacing. Support of the Air Force Office of Scientific Research/Army Research Office (Grant DAAG29-81-K-0033) is acknowledged. H. Bartelt is on leave from the Physikalisches Institut der Universität Erlangen-Nürnberg, Erlangen, West Germany.

7. REFERENCES

1. S. K. Case, P. R. Haugen, and O. J. Lokberg, Appl. Opt. 20(15), 2670(1981).
2. S. K. Case and P. R. Haugen, Opt. Eng. 21(2), 352(1982).
3. B. J. Chang and C. D. Leonard, Appl. Opt. 18(14), 2407(1979).
4. P. R. Haugen, H. Bartelt, and S. K. Case, to be published.
5. O. Bryngdahl, J. Opt. Soc. Am. 64, 1092(1974).
6. A. W. Lohmann, *Optical Information Processing*, Physikalisches Institut der Universität Erlangen-Nürnberg, Erlangen, West Germany (1978).

2. List of Scientific Personnel

The following individuals contributed to the research effort supported by this grant.

1. Steven K. Case, Associate Professor, Electrical Engineering Department, Principle Investigator.
2. Dr. Hartmut Bartelt, Visiting Research Scientist (1981-82).
3. Brian Adams, Research Assistant, (MS, 9/81).
4. Paul Haugen, Research Assistant, (MS, 6/82).
5. Daniel Hulsey, Research Assistant (MS, 6/82).
6. Chris Henze, Research Assistant, (MS, 8/83).
7. Tim Grotjohn, Research Assistant.
8. Larry Konicek, Research Assistant (MS candidate).
9. Rolf Enger, Research Assistant (Ph.D., 8/83).
10. Ron Indeck, Research Assistant.
11. Jeff Jalkio, Research Assistant, Ph.D. Candidate.
12. Richard Kim, Research Assistant, MS Candidate.

3. List of Publications

1. S. K. Case, "Wavelength Coding for Image Transmission through Aberrating Media," Opt. Lett. 6, 311 (1981).
2. S. K. Case, P. R. Haugen and O. J. Lokberg, "Multi-Facet Holographic Optical Elements for Wavefront Transformations," Appl. Opt. 20, 2670 (1981).
3. S. K. Case and P. R. Haugen, "Partitioned Holographic Optical Elements," Opt. Engin. 21, 352 (1982).
4. S. K. Case and P. R. Haugen, "Multifacet Holographic Optical Elements," Proceedings of NASA Optical Information Processing Conference, R. Segura, ed., NASA Langley Research Center, Hampton, VA 23665, August 1981.
5. H. Bartelt and S. K. Case, "Spatial Frequency Pseudo-Coloring with Binary Filters", Opt. Commun. 42, 162 (1982).
6. H. Bartelt and S. K. Case, "High Efficiency Hybrid Computer Generated Holograms," Appl. Opt. 21, 2886 (1982).
7. B. Adams and S. K. Case, "Electro-Optic Imaging System using Wavelength Coding", Appl. Opt. 22, 2026 (1983).
8. D. E. Hulsey and S. K. Case,"A Fiber Optic Imaging System using Wavelength Coding", Appl. Opt. 22, 2029 (1983).
9. P. R. Haugen, H. Bartelt, and S. K. Case, "Image Formation by Multifacet Holograms", Appl. Opt. 22, 2822 (1983).
10. H. Bartelt and S. K. Case, "Coordinate Transformation via Multifacet Holographic Optical Elements," Opt. Engin. 22, 497 (1983).
11. R. C. Enger and S. K. Case, "High Frequency Holographic Transmission Gratings in Photoresist", J. Opt. Soc. Am. 73, 1113 (1983).

12. C. P. Henze and S. K. Case, "A Polychromatic Laser Light Source", Rev. Sci. Instruments 54, 1334 (1983).

13. R. C. Enger and S. K. Case, "Optical Elements with Ultra High Spatial Frequency Surface Corrugations", Appl. Opt. 22, 3220 (1983).

14. S. K. Case and P. R. Haugen, "High Efficiency Multifacet Holographic Optical Elements for Image Formation", Proceedings of SPIE Conference on Computer Generated Holography, Vol. 437, p. 137 (Aug. 25-26, 1983).

15. Invited Paper. S. K. Case, H. O. Bartelt, P. R. Haugen and L. Konicek, "Multi-Facet Holographic Optical Elements", Laser Institute of America Conference Proceedings, Nov. 1983.

16. L. Konicek and S. K. Case, "Information Encoding Systems Employing Multifaceted Volume Holograms", Opt. Commun. 49, 397 (1984).

4. List of Presentations

The following oral presentations at meetings and conferences described research supported by this grant.

1. S. K. Case, P. Haugen, O. J. Lokberg, "Multi-Facet Holographic Optical Elements", Annual Meeting OSA, October, 1980. Abstract: J. Opt. Soc. Am. 70, 1625 (1980).
2. S. K. Case and P. R. Haugen, "Multifacet Holographic Optical Elements," NASA Optical Information Processing Conference, Hampton, VA, August 1981.
3. S. K. Case and P. R. Haugen, "Image Formation via Multi-Facet Holograms," International Commission for Optics Conference, Graz, Austria, September 1981.
4. Invited paper. S. K. Case, "Multifacet Holographic Optical Elements", Gordon Research Conference on Coherent Optics and Holography, June, 1982.
5. S. K. Case and H. Bartelt, "High Efficiency Hybrid Computer Generated Holograms", Annual Meeting OSA, October, 1982. Abstract: J. Opt. Soc. Am. 72, 1751 (1982).
6. S. K. Case and S. Arnold, "Computer Generated Hologram Facilities," Information Processing and Holography Technical Group Meeting, Annual Meeting of OSA, Tucson, AZ, Oct. 1982.
7. S. K. Case, H. Bartelt, C. Henze and D. Hulsey, "Wavelength Coded Image Transmission in Fiber Optic Systems," OSA Optical Fiber Communication Conference, New Orleans, Feb. 1983. Abstract: Technical Digest, Topical Meeting on Optical Fiber Communication, Optical Society of America, p. 60.
8. H. Bartelt and S. K. Case, "Holographic Optical Elements in Dichromated Gelatin", Deutsch Gesellschaft für Angewandte Optik (Annual Meeting), Darmstadt, West Germany, May, 1983.

9. S. K. Case and P. R. Haugen, "High Efficiency Multifacet Holographic Optical Elements for Image Formation", S.P.I.E. Conference on Computer Generated Holograms, San Diego, Aug. 26, 1983.

10. R. C. Enger and S. K. Case, "Holograhic Optical Elements with Ultrahigh Spatial Frequencies", Annual Meeting OSA, October 1983.

11. Invited Paper. S. K. Case, H. O. Bartelt, P. R. Haugen, and L. Konicek, "Multi-Facet Holographic Optical Elements", Laser Institute of America Conference, Los Angeles, Nov. 1983.

12. Invited Paper. S. K. Case, "Efficient Holographic Optical Elements", DARPA Conference of Diffractive Optics, La Jolla, CA, May 1984.